*Environmental Health Perspectives*
*Vol. 85, pp. 249–274, 1990*

# Nonneoplastic Nasal Lesions in Rats and Mice

by Thomas M. Monticello,* Kevin T. Morgan,* and Linda Uraih†‡

**Rodents are commonly used for inhalation toxicology studies, but until recently the nasal passages have often been overlooked or only superficially examined. The rodent nose is a complex organ in which toxicant-induced lesions may vary, depending on the test compound. A working knowledge of rodent nasal anatomy and histology is essential for the proper evaluation of these responses. Lack of a systematic approach for examining rodent nasal tissue has led to a paucity of information regarding nonneoplastic lesions in the rodent nose. Therefore, slides from the National Toxicology Program (NTP) and the Chemical Industry Institute of Toxicology (CIIT) were examined, and the literature was reviewed to assemble the spectrum of nonneoplastic rodent nasal pathology. Presented are lesions associated with the various types of epithelia lining the rodent nasal cavity plus lesions involving accessory nasal structures. Even though there are anatomic and physiologic differences between the rodent and human nose, both rats and mice provide valuable animal models for the study of nasal epithelial toxicity, following administration of chemical compounds.**

## Introduction

Although the rodent is a commonly used laboratory animal for inhalation toxicology studies, there is a paucity of information in the literature regarding nonneoplastic lesions in the nasal cavity. This lack of data may be attributed to the fact that the nasal cavity is often overlooked or examined superficially. Since the nose is highly complex and the nature of toxicant-induced lesions may vary with the test compound (Table 1) (*1–14*), a working knowledge of nasal anatomy and histology is essential for the proper evaluation of these responses. Following the published methodology for examination of the rodent nose (*15*), the nasal cavity has received more systematic attention in toxicology studies.

The objective of this paper is to describe the more common nonneoplastic lesions of the rodent nose that may be encountered during the evaluation of a toxicology study. Lesions involving the various types of epithelia lining the nasal cavity and lesions of the major accessory nasal structures such as glands, the vomeronasal organ, nasolacrimal duct, bone, and maxillary recess will be addressed.

## Materials and Methods

Material for this review was obtained from the National Toxicology Program (NTP) archives and previous rodent inhalation studies conducted by the Chemical Industry Institute of Toxicology (CIIT). Study pathologists at CIIT or at various facilities under contract to the NTP supervised the necropsies and conducted the initial histopathological examinations. Routine fixation and handling techniques were used. The nose was removed from the carcass, fixed in 10% buffered formalin, cut transversely at two to five representative levels, embedded in paraffin, and sectioned at 5 to 6 $\mu$m. All slides were routinely stained with hematoxylin and eosin and with special stains where appropriate. For the present study, all nasal sections were reevaluated without reference to previous diagnoses. Levels of the nasal cavity were generally similar to those described by Young (*15*).

## Results

### Nasal Epithelium

***Stratified Squamous Epithelium.*** The nasal vestibule, which is the most anterior portion of the rat nasal cavity, is lined by stratified squamous epithelium, as is the floor of the ventral meatus, anterior to the incisive ducts. Squamous epithelium is fairly resistant to the effects of inhaled toxicants; however, with certain irritants such as dimethylamine (DMA), lesions may be observed (*3*). Acute lesions of the squamous epithelium include erosion or ulceration (Plate 1), with or without an accompanying inflammatory cell component consisting primarily of neutrophils. Subacute or chronic lesions in the squamous epithelium, such as hyperplasia and hyperkeratosis, may represent defensive or adaptive responses. As in the dermis, prolonged epithelial hyperplasia may lead to rete-ridge formation, an irregular

*Chemical Industry Institute of Toxicology, Research Triangle Park, NC 27709.
† Present address: Pfizer Central Research, Bldg. 174, Eastern Point Rd., Groton, CT 06340.
‡ National Institute of Environmental Health Sciences, Research Triangle Park, NC 27709.
Address reprint requests to T. M. Monticello, CIIT, P.O. Box 12137, Research Triangle Park, NC 27709.

**Table 1. Nonneoplastic nasal lesions in rats and mice exposed to various chemical toxicants.[a]**

| Chemical | Epithelial type | | | Reference |
|---|---|---|---|---|
| | Squamous | Respiratory | Olfactory | |
| Methyl bromide | — | — | DEG, ULC | (*1*) |
| Dimethylamine | ULC, NEC | DEG, ERO, INF, MET | DEG | (*2,3*) |
| 1,2-Epoxybutane | — | INF, HYP, MET | DEG | (*4*) |
| 3-Trifluoromethyl pyridine | — | | DEG | (*5*) |
| 1,2-Dibromoethane | — | HYP, MET | DEG, NEC | (*6*) |
| Acetaldehyde | — | HYP, INF, MET | DEG, HYP, MET | (*7–9*) |
| Formaldehyde | — | DEG, INF, ERO, ULC, HYP, MET | — | (*10*) |
| Acrolein | — | INF, NEC, MET | — | (*11*) |
| Chlorine | — | INF, ERO, ULC, NEC, MET | ULC, NEC | (*12*) |
| Sulfur dioxide | — | DEG, NEC | — | (*13*) |
| 3-Methylfuran | — | — | NEC | (*14*) |

[a]Key: ULC, ulceration; NEC, necrosis; DEG, degeneration; ERO, erosion; INF, inflammation; MET, metaplasia; HYP, hyperplasia.

hyperplasia which results in pegs of squamous epithelium that project down into the underlying lamina propria (Plate 2).

Lesions confined to the ventral meatus are uncommon but include ulceration, which is seen following hydrogen chloride exposure (*16*) and focal squamous hyperplasia (Plate 3). The incisive ducts, lined entirely by stratified squamous epithelium, are normal anatomical structures that provide direct communication between the oral and nasal cavities (Plate 4). They extend from the floor of the ventral meatus through the hard palate and exit into the oral cavity at the incisive papilla. Food material may become lodged in these ducts, eliciting an inflammatory reaction. Other lesions present in this location, however, are rare.

***Respiratory Epithelium.*** Despite its frequent characterization as pseudostratified ciliated columnar epithelium, the respiratory epithelium exhibits varied morphologic characteristics that differ from area to area (*17*). Physiologic and scanning electron microscopy studies have demonstrated a marked variation in the density of the ciliated cell population (*18,19*), and ciliary length (*19*) throughout the nasal cavity. Starting just posterior to the squamous epithelium of the vestibule and extending to the anterior one-third of the maxilloturbinate (the transitional zone), the lateral aspect of the nasoturbinate and the lateral wall are covered by a thin zone of pseudostratified cuboidal epithelium, composed of cuboidal and basal cells (*17*) (Plates 5 and 6). Rare secretory and ciliated cells are randomly found in these areas. The middle third of the respiratory epithelium has more ciliated cells than the anterior third (*19*), while the distal third consists of ciliated epithelium with secretory cells.

Acute inflammation of the rodent nasal mucosa is a common sequelum to toxic insult, with the resulting lesions being similar to those occurring in any other tissue. The main characteristic of acute inflammation in the rodent nasal cavity is edema of the lamina propria (Plate 7), which is often associated with an eosinophilic homogeneous serous transudate that fills the nasal airways. Emigration of leukocytes, primarily neutrophils, follows. Normally, few inflammatory cells are present in the respiratory epithelium. However, following an acute respiratory epithelial insult, increased numbers may be observed migrating through the epithelium, resulting in a suppurative rhinitis (Plate 8). Suppurative rhinitis is commonly associated with exposure to certain nasal toxicants and may be attributed to opportunist infections following enhanced susceptibility. Suppurative rhinitis can also be seen in association with fungal infections and foreign bodies.

A number of noninflammatory changes are frequently observed in the respiratory epithelium including loss of cilia, cellular swelling, epithelial cell bleb formation, separation of cells, and finally exfoliation (*20*). The lateral wall and the free margins of both the nasoturbinates and maxilloturbinates often exhibit the first evidence of toxic nasal insult after exposure to many irritant gases. A continued loss of cells results in erosion (Plate 9) and ulceration, which is often accompanied by a serocellular exudate containing neutrophils (Plate 10). Following erosion or ulceration of the epithelium, cellular debris admixed with fibrin may become free in the nasal lumen and act as a scaffold for regenerating epithelial cells, resulting in fusion of turbinates to adjacent structures such as the lateral wall (Plate 11) or septum. Commonly occurring nasal adhesions include the following: nasoturbinate with nasoturbinate; nasoturbinate with maxilloturbinate; nasoturbinate with lateral wall; and maxilloturbinate with lateral wall.

Secretory cell and respiratory epithelial cell hypertrophy/hyperplasia are common responses to certain gaseous irritants such as cigarette smoke (*21*), formaldehyde (*20*), and ammonia (*22*) (Plates 12–14). Secretory cell hyperplasia and hypertrophy may provide increased amounts of mucus to the nasal airways and may thus represent an adaptive response. Concurrent with inflammation, intraepithelial microabcesses may form in association with the transmigration of neutrophils through hyperplastic epithelium (Plate 14). Prolonged respiratory epithelial cell hyperplasia is associated with mucosal folding (Plate 13) and glandlike invagination of the mucosa, forming intraepithelial crypts termed pseudoglands (*23*). The mucosal folding in the hyperplastic response may be a result of increased epithelial

surface length (*24*). The mucosal surface of the posterior ventral margin of the nasoturbinate is normally folded and should not be interpreted as epithelial hyperplasia (*25*).

Adaptive squamous metaplasia of the respiratory epithelium is a well-documented reaction to many types of injury (*26,27*). It is a common response observed in the rodent nasal passages following chronic exposure to cytotoxic irritants (Plates 15 and 16). Areas of adaptive squamous metaplasia may be confined to certain locations within the nasal cavity or may be quite diffuse, depending on the particular chemical compound and duration of exposure. This metaplastic change is characterized by the replacement of the more susceptible respiratory epithelium by squamous epithelium, which is more resistant to injury by many inhaled toxicants. An early feature of squamous metaplasia is disorganization of the normal respiratory epithelium, with altered polarity of the more superficial cells towards a horizontal orientation with respect to the basal lamina. Squamous metaplasia may continue to progress, evidenced by both cellular stratification and increased numbers of surface squames, eventually forming a mature squamous epithelium in place of the original respiratory epithelium. The metaplastic epithelium may be either keratinized or nonkeratinized. Keratinization can be so severe that plugs of keratin occlude portions of the nasal cavity, resulting in dyspnea and even death of the animal. Examples of irritants that induce hyperplasia, squamous metaplasia and keratinization (Plate 17) include acetaldehyde (*7,8*), formaldehyde (*10*), and acrolein (*11*).

Squamous metaplasia with atypia (sometimes termed dysplasia), is often regarded as a possible precursor of neoplasia (*27*). This lesion is characterized by one or more of the following features: recognizable stratification with or without keratinization, increased numbers of mitotic figures, occurrence of atypical mitoses, cellular pleomorphism, variable staining affinity, and individual cell keratinization (dyskeratosis) in the deeper layers (*27*). Histological differences in dysplasia are mainly quantitative, i.e., slight atypia exhibits a few of the aforementioned features (Plate 18), whereas severe atypia exhibits most or all of them.

Currently, immunohistochemical techniques for detecting certain epidermal proteins, such as involucrin and subtypes of keratin, are used as aids in detecting preneoplastic and neoplastic lesions in human nasal biopsies (*28*). It is hoped that similar immunohistochemical techniques may be developed as an aid in differentiating preneoplastic from neoplastic respiratory epithelial lesions in rodent tissues.

Miscellaneous lesions encountered in the respiratory mucosa of the nasal cavity include intracellular eosinophilic globules, corpora amylacea, and deposits of homogeneous eosinophilic material in the lamina propria of the ventral septum. Eosinophilic globules (also termed "intracytoplasmic hyaline droplets") (Plate 19) are normally found in low numbers in control rats and mice, and increase with age (unpublished observations). They increase in quantity and severity following chronic exposure to certain toxicants such as DMA (*2*), perhaps constituting an adaptive response. Eosinophilic globules stain brightly eosinophilic on hematoxylin and eosin, are negative for both neutral and acidic mucosubstances, and are negative for a number of special stains (Table 2). By transmission electron microscopy, cells with eosinophilic globules exhibit massively dilated cisternae of the rough endoplasmic reticulum, which contain homogenous electron-dense material (*29*). The exact composition of this material has not yet been determined but may represent proteinaceous secretory material that accumulates in the cell. By light microscopy, similar eosinophilic droplets are found in respiratory secretory cells and olfactory sustentacular cells (Plate 20). The lumen of nasal glands with eosinophilic globules in glandular epithelium often contain eosinophilic crystals (Plate 21).

Small laminated basophilic bodies (corpora amylacea) are occasionally found in the respiratory mucosa (Plate 22) and the lumen of nasal glands of control or treated mice and rats, and these bodies have been reported in association with eosinophilic globules in mice chronically exposed to DMA. Another common incidental finding in rodents is the presence of homogeneous eosinophilic material in the lamina propria of the ventral septal area (Plate 23). This material has an amyloidlike appearance in hematoxylin and eosin stained sections, but it stains negatively using the Congo red method. As shown in Table 2, this material stains positive for neutral mucosubstances. The exact nature and significance of this material remains to be determined.

**Table 2. Summary of histochemical findings.**

| Stain | Eosinophilic globules[a] | Eosinophilic material in septum[a] |
|---|---|---|
| Periodic acid-Schiff | – | + |
| With digest | – | + |
| Without digest | – | – |
| Alcian blue (pH 2.5) | – | – |
| Von Kossa | – | – |
| Mucicarmine | – | – |
| PTAH | – | – |
| Masson's trichrome | – | – |
| Congo red | – | – |
| Toluidine blue | – | – |

[a]See text.

***Olfactory Epithelium.*** The line of demarcation between the respiratory and olfactory epithelium is irregular and generally abrupt throughout the nasal cavity (*17*). The region of olfactory epithelium in the rodent nose begins in the wall of the dorsal meatus at the level of the vomeronasal organ and extends posteriorly to cover the ethmoid turbinates. Olfactory epithelium consists of three major cell types: basal cells, sustentacular cells (supporting cells), and sensory cells. Basal cells are located in the lower third of the epithelium adjacent to the basement membrane. The upper third of the olfactory epithelium is composed largely of sustentacular cells, and the cell bodies of the olfactory sensory neurons are located in the middle third of the epithelium between the supporting cells and basal cells. Bowman's glands are located in the subjacent lamina propria. The ducts of these glands extend through the olfactory epithelium opening at the epithelial surface. It is important to be familiar with the normal structure of the olfactory epithelium since the height of the mucosa, the number of sensory cells, number and size of olfactory nerves, and features of Bowman's glands display considerable regional (*25*) and species variability.

The most common location where olfactory epithelial toxicity is observed in rats and mice in inhalation studies is the anteriodorsal extension of the olfactory mucosa into the dorsal meatus (*25*). Acute olfactory lesions can be induced by a variety of compounds and may vary depending on the target cell involved. Methyl bromide-exposed rats first show degenerative olfactory epithelial changes involving the sustentacular cells (*30*). In contrast, rats and mice exposed to DMA consistently exhibit olfactory epithelial atrophy (Plate 24) resulting from sensory cell degeneration (*2*). Complete ulceration or necrosis of the olfactory mucosa follows exposure to compounds such as chlorine (*12*), sulfur dioxide (*13*), 3-methylfuran (*14*), methyl bromide (*1*), and tobacco-specific nitrosamines (*31*).

Regeneration of the olfactory epithelium may be noted as hyperplasia of presumed basal cells (Plate 25), which become stratified. These cells have moderate eosinophilic cytoplasm and round-to-oval nuclei. Proliferating basal cells may form small aggregates or intraepithelial rosette-like structures (Plate 26), and have been observed in the F344 rat treated with nitrosomethylpiperazine (*32*), and other chemicals.

Repair of the olfactory epithelium can result in squamous or respiratory metaplasia (Plate 27) or in complete recovery of olfactory epithelium. Respiratory metaplasia has been reported as an aging lesion in rats (*3*). Factors which influence the specific type of differentiation that occurs during recovery from olfactory toxicity have yet to be determined. Feron et al. (*33*) states that olfactory epithelial replacement by a respiratorylike mucosa possibly represents olfactory epithelium that has lost its sensory cells. It then consists of only basal and sustentacular cells, the latter of which may be mistaken for ciliated cells. Upon closer examination, however, these cell types may be differentiated by the location of their nucleus. Ciliated respiratory columnar cells have a mid- or basally positioned nucleus, while the nucleus of sustentacular cells is located apically. Further studies are needed to determine the actual histogenesis of olfactory epithelial recovery and metaplasia in the rodent.

Other nonneoplastic lesions of the nasal olfactory mucosa in experimental rodents include basement membrane mineralization and degeneration of Bowman's glands (*31*) and olfactory nerves. Small aggregates of mineralized debris in the mucosa (corpora amylacea), and accumulation of eosinophilic globules in sustentacular cells (*25*) are lesions that can occur in both control or chemically treated animals.

## Nasal Glands and Maxillary Sinus

Nasal glands, located in the lamina propria, are mucous, serous or mixed. These glands play an important role in the production of nasal secretions that protect the upper airways. Detailed anatomical and histochemical studies of the rodent nasal glands have been reported (*34,35*). Most glands in the lateral wall of the rat are situated around the maxillary sinus. In the ventral half of the nasal septum they are densely arranged (*35*), while the dorsal half of the septum contains fewer glands. Bowman's glands are found only in olfactory mucosa and provide secretory material which keeps the epithelial surface moist (*36*). Familiarity with the distribution of these structures in the rodent nose is therefore important for the interpretation of changes such as glandular hyperplasia, atrophy, and recognition of pseudogland formation.

Acute inflammatory lesions of the nasal glands often accompany rhinitis and may result in glandular dilatation and plugging by inflammatory cells (Plate 28). Glandular hyperplasia may result following chronic irritation and has been reported by Reznik et al. (*37*) in rats fed diets containing *p*-cresidine. Squamous metaplasia (Plate 28), degeneration, or necrosis of glands (Plate 28) can occur following the administration of certain toxic compounds such as 1,2-dibromo-3-chloropropane (*38*). Atrophy of glands may present either as an aging lesion or in association with glandular necrosis. Degeneration and necrosis of Bowman's glands were prominent findings in a study with the tobacco-specific nitrosamine 4-(*N*-methyl-*N*-nitrosamino)-1-(3-pyridyl-)-1-butanone (NNK) (*31*).

The maxillary sinus (often termed "recess") is the only paranasal sinus in the rat. The two glandular systems related to this sinus are the lateral nasal gland (Steno's gland) and the maxillary gland (*39*). These glands completely surround the sinus and occupy most of the submucosa. Necrosis of Steno's gland was seen following the administration of NNK (*31*) (Plate 29). The maxillary sinus is primarily lined by pseudostratified ciliated columnar epithelium with rare goblet cells. The portion of the epithelium that covers the maxillary gland resembles a simple columnar epithelium. The maxillary sinus is a common site for a suppurative exudate usually in association with a severe neutrophilic rhinitis. Lesions of the

epithelial lining of the sinus include hyperplasia and squamous metaplasia.

## Blood Vessels

Vascular congestion and/or hyperemia of the nasal vessels is a common occurrence in euthanized animals and is related to terminal passive congestion. Telangiectasia of venous sinuses in the nasal cavity may be seen as a treatment-related lesion. An uncommon vascular lesion encountered in the rodent nasal cavity, however, is thrombosis (Plate 30). Thrombi, reported in the majority of vessels in the anterior nasal cavity in a chemical inhalation study (*3*), were not present in vessels of the posterior nasal cavity, nor were they present in the major organs examined. This distribution of nasal thrombi (i.e., confined to the anterior nasal cavity) suggests a localized vascular insult induced by the inhaled compound.

## Bone

Lesions involving the nasal turbinate bones are infrequently reported. Certain inhaled compounds which are highly irritative, such as DMA, can cause atrophy of the turbinates in the nasal vestibule and septal perforation (*3*). Severe ulceration of the overlying mucosa can result in the exposure of the turbinate bone and bone necrosis (Plate 31). Osteofibrosis is a general reaction of the rodent turbinate bones to injury, either by toxic insult or inflammation.

Osteofibrosis is characterized by a loss of the cancelleous bone of the turbinates and a proliferation of osteoprogenitor or fibroblastlike cells near the periosteal surface (Plate 32). The basic defect is believed to be in the osteoblasts, which either produce an altered osteoid or have a decrease in osteoid synthesis. Osteoclasts are not significantly changed in number. Osteofibrosis has been reported in control animals, but it can increase in frequency following the administration of some chemicals.

Osteopetrosis (also termed hyperostosis), is a systemic skeletal condition in which bone tissue accumulates. Osteopetrosis can involve the bones of the skull and turbinates (Plate 33), resulting in a marked thickening of the naso- and maxilloturbinates, and is oftentimes associated with atrophy of the nasal mucosa. The proposed pathogenesis of hyperostosis in the rat involves reduced bone resorption because of diminished osteoclast function (*40*). Severe necrosis with an associated remodeling of the nasal turbinates (Plate 34) can occur following exposure to certain chemicals such as 3-methylfuran (*14*). Following exposure to this chemical, extensive necrosis leads to remodeling of the turbinates and an associated fibrosis and partial occlusion of the nasal passages (*14*).

## Accessory Nasal Structures

The vomeronasal organ (Jacobson's organ) is ventral to the nasal septum at the level of the nasal cavity, just posterior to the upper incisor teeth (Plate 35). This paired organ is lined medially by olfactory epithelium that overlies nonmyelinated nerves. The lateral aspect of Jacobson's organ is lined by pseudostratified ciliated columnar epithelium. Low numbers of neutrophils are commonly noted in transepithelial migration at this site. However, associated with a neutrophilic rhinitis, a suppurative exudate may fill the vomeronasal organ lumen. Degeneration and vacuolation of the olfactory epithelial portion of Jacobson's organ may indicate early autolytic change in the rat nasal cavity.

The paired nasolacrimal ducts originate from the medial canthus of the eye and extend cranio-ventrally to their anterior terminus in the nasal vestibule. Depending on the level of the nasal cavity examined, the nasolacrimal ducts can be found dorsally (at the level near their origin); laterally (to the roots of the incisor teeth at the level of the incisive papilla); ventrally (to the maxilloturbinate); or ventromedially (to the roots of the incisor teeth in the vestibule). The lining of these ducts also varies from stratified squamous to low columnar epithelium, depending on the level of the nasal cavity examined, and it has been described as a transitional epithelium (*41*). At the origin of these ducts, small subepithelial lymphoid aggregates are usually present. Lesions in the lining epithelium include inflammatory cell transmigration, epithelial hyperplasia with exfoliation, and squamous metaplasia with or without keratinization (Plate 36).

## Teeth

The roots of the upper incisor teeth in rats and mice extend posteriorly in the lateral aspect of the skull and play an important role in the shaping of the anterior nasal passages (*42*). Rodent incisor teeth have persistent pulps and grow throughout the life of the animal. Dental dysplasia (odontodysplasia), the disorderly growth of tooth bud elements, is a frequently reported lesion (Plate 37). Dysplastic incisor teeth in the rodent may become so large as to partially occlude the nasal passages (Plate 38). When dental dysplasia occurs following impaction by a foreign body (i.e., food material or hair), inflammation and necrosis of the tooth can result, which may subsequently lead to a rhinitis (*43*).

# Conclusions

The nasal cavity has become a routine organ for histopathological examination in rodent inhalation toxicity studies. Knowledge, therefore, of nasal anatomy, histology, lesion distribution, and commonly encountered lesions is essential for proper evaluation of the rodent nose. It should be realized that the anatomical and physiological differences of the rodent nose, as compared to humans, may influence the distribution of lesions within the upper and lower respiratory tract. Even with these species differences considered, the rodent remains a valuable model for studying pathologic injury of the respiratory and olfactory mucosa following the administration of chemical compounds.

The authors would like to thank M. Morris and D. Joyner and their technical assistance and D. Farnell for providing helpful comments and references following the meeting.

## REFERENCES


1. Hurtt, M. E., Morgan, K. T., and Working, P. K. Histopathology of acute toxic responses in selected tissues from rats exposed by inhalation to methyl bromide. Fundam. Appl. Toxicol. 9: 352–365 (1987).
2. Buckley, L. A., Morgan, K. T., Swenberg, J. A., James, R. A., Hamm, T. E., and Barrow, C. S. The toxicity of dimethylamine in F-344 rats and B6C3F1 mice following a 1-year inhalation exposure. Fundam. Appl. Toxicol. 5: 341–352 (1985).
3. Gross, E. A., Patterson, D. L., and Morgan, K. T. Effects of acute and chronic dimethylamine exposure on the nasal mucociliary apparatus of F-344 rats. Toxicol. Appl. Pharmacol. 90: 359–376 (1987).
4. Dunnick, J. K., Eustis, S. L., Piegorsch, W. W., and Miller, R. A. Respiratory tract lesions in F344/N rats and B6C3F mice after inhalation exposure to 1,2-epoxybutane. Toxicology 50: 69–82 (1988).
5. Gaskell, B. A., Hext, P. M., Pigott, G. H., Hodge, M. C. H., and Tinston, D. J. Olfactory and hepatic changes following inhalation of 3-trifluromethyl pyridine in rats. Toxicology 50: 57–68 (1988).
6. Reznik, G., Stinson, S. F., and Ward. J. M. Respiratory pathology in rats and mice after inhalation of 1,2-dibromo-3-chloropropane or 1,2 dibromoethane for 13 weeks. Arch. Toxicol. 46: 233–240 (1980).
7. Kruysse, A., Feron, V. J., and Til, H. P. Repeated exposure to acetaldehyde vapor. Studies in Syrian golden hamsters. Arch. Environ. Health. 31: 449–452 (1975).
8. Feron, V. J., Kruysse, A., and Woutersen, R. A. Respiratory tract tumors in hamsters exposed to acetaldehyde vapor alone or simultaneously to benzo(a)pyrene or diethylnitrosamine. Eur. J. Cancer Clin. Oncol. 18: 13–31 (1982).
9. Appelman, L. M., Woutersen, R. A., and Feron, V. J. Inhalation toxicity of acetaldehyde in rats. I. Acute and subacute studies. Toxicology 23: 293–307 (1982).
10. Kerns, W. D., Pavkov, K. L., Donofrio, D. J., Gralla, E. J., and Swenberg, J. A. Carcinogenicity of formaldehyde in rats and mice after long-term inhalation exposure. Cancer Res. 43: 4382–4392 (1983).
11. Feron, V. J., Kruysse, A., Til, H. P., and Immel, H. R. Repeated exposure to acrolein vapor: subacute studies in hamsters, rats and rabbits. Toxicology 9: 47–57 (1978).
12. Jiang, X. Z., Buckley, L. A., and Morgan, K. T. Pathology of toxic responses to the RD50 concentration of chlorine gas in the nasal passages of rats and mice. Toxicol. Appl. Pharmacol. 71: 225–236 (1983).
13. Giddens, W. E., and Fairchild, G. A. Effects of sulfur dioxide on the nasal mucosa of mice. Arch. Environ. Health 25: 166–173 (1972).
14. Haschek, W. M., Morse, C. C., Boyd, M. R., Hakkinen, P. J., and Witschi, H. P. Pathology of acute inhalation exposure to 3-methylfuran in the rat and hamster. Exp. Mol. Pathol. 39: 342–354 (1983).
15. Young, J. T. Histopathologic examination of the rat nasal cavity. Fundam. Appl. Toxicol. 1: 309–312 (1981).
16. Buckley, L. A., Jiang, X. Z., James, R. A., Morgan, K. T., and Barrow, C. S. Respiratory tract lesions induced by sensory irritants at the RD50 concentration. Toxicol. Appl. Pharmacol. 74: 417–429 (1984).
17. Monteiro-Riviere, N. A., and Popp, J. A. Ultrastructural characterization of the nasal respiratory epithelium in the rat. Am. J. Anat. 169: 31–43 (1984).
18. Popp, J. A., and Martin, J. T. Surface topography and distribution of cell types in the rat nasal respiratory epithelium: scanning electron microscopic observations. Am. J. Anat. 169: 425–436 (1984).
19. Morgan, K. T., Jiang, X. Z., Patterson, D. L., and Gross, E. A. The nasal mucociliary apparatus. Correlation of structure and and function in the rat. Am. Rev. Respir. Dis. 130: 275–281 (1984).
20. Monteiro-Riviere, N. A., and Popp, J. A. Ultrastructural evaluation of acute nasal toxicity in the rat respiratory epithelium in response to formaldehyde gas. Fundam. Appl. Toxicol. 6: 251–262 (1986).
21. Vidić, B., Washington, D. C., Rana, M. W., and Bhagat, B. D. Reversible damage of rat upper respiratory tract caused by cigarette smoke. Arch. Otolaryngol. 99: 110–113 (1974).
22. Broderson, J. R., Lindsey, J. R., and Crawford, J. E. The role of environmental ammonia in respiratory mycoplasmosis of rats. Am. J. Pathol. 85: 115–130 (1976).
23. Gopinath, C., Prentice, D. E., and Lewis, D. J., Eds. The Respiratory System, Vol. 13. Atlas of Experimental Toxicological Pathology. MTP Press Limited, Lancaster, UK, 1988, pp. 23–41.
24. Jeffery, P. K., and Reid, L. M. The respiratory mucous membrane. In: Respiratory Defense Mechanisms, Part 1 (J. B. Brain, D. F. Proctor, and L. M. Reid, Eds.), Marcel Dekker, Inc., New York, 1977, pp. 193–229.
25. Jiang, X. Z., Morgan, K. T., and Beauchamp, R. O., Jr. Histopathology of acute and subacute nasal toxicity. In: Toxicology of the Nasal Passages (C. S. Barrow, Ed.), Hemisphere Pub. Corp., Washington, DC, 1986, pp. 51–65.
26. Becci, P. J., McDowell, E. M., and Trump, B. F. The respiratory epithelium. IV. Histogenesis of epidermal metaplasia and carcinoma *in situ* in the hamster. J. Nat. Cancer Inst. 61: 577–586 (1976).
27. Klein-Szanto, A. J. P., Topping, D. C., Heckman, C. A., and Nettesheim, P. Ultrastructural characteristics of carcinogen-induced dysplastic changes in tracheal epithelium. Am. J. Pathol. 98: 83–100 (1981).
28. Klein-Szanto, A. J. P., Boysen, M., and Reith, A. Keratin and involucrin in preneoplastic and neoplastic lesions. Arch. Pathol. Lab. Med. 111: 1057–1061 (1987).
29. Popp, J. A., Morgan, K. T., Everitt, J., Jiang, X. Z., and Martin, J. T. Morphologic changes in the upper respiratory tract of rodents exposed to toxicants by inhalation. In: Microbeam Analysis (A. D. Romig, Jr., and W. F. Chambers, Eds.), San Francisco Press, Inc., San Francisco, CA, 1986, pp 581–582.
30. Thomas, D. A., Lyght, O., and Morgan, K. T. Ultrastructural changes in olfactory epithelium of rats following inhalation exposure to methyl bromide (abstract). Toxicologist 1: 250 (1988).
31. Belinsky, S. A., Walker, V. E., Maronpot, R. R., Swenberg, J. A., and Anderson, M. W. Molecular dosimetry of DNA adduct formation and cell toxicity in rat nasal mucosa following exposure to the tobacco specific nitrosamine 4-(N-methyl-N-nitrosamino)-1-(3-pyridyl-1)-1-butanone and their relationship to induction of neoplasia. Cancer Res. 47: 6058–6065 (1987).
32. Reznik-Schüller, H. M. Nitrosamine-induced nasal cavity carcinogenesis. In: Nasal Tumors in Animals and Man, Experimental Nasal Carcinogenesis, Vol. 3 (G. Reznik, and S. F. Stinson, Eds.) CRC Press, Boca Raton, FL, 1983, pp. 47–74.
33. Feron, V. J., Wortersen, R. A., and Spit, B.J. Pathology of chronic nasal toxic responses including cancer. In: Toxicology of the Nasal Passages (C. S. Barrow, Ed.), Hemisphere Pub. Corp., Washington, DC, 1986, pp. 67–75.
34. Katz, S., and Merzel, J. Distribution of epithelia and glands of the nasal septum mucosa in the rat. Acta. Ana. 99:58–66 (1977).
35. Klaassen, A. B. M., Kuijpers, W., and Denuce, J. M. Morphological and histochemical aspects of the nasal glands in the rat. Anat. Anz. 149–51–63 (1981).
36. Uraih,
37. Reznik, G., Reznik-Schüller, H. M., Hayden, D. W., Russfield, A., and Krishna Murthy, A. S. Morphology of nasal cavity

neoplasms in F-344 rats after chronic feeding of p-cresidine, an intermediate of dyes and pigments. Anticancer Res. 1: 279–286 (1981).
38. Reznik, G., Reznik-Schüller, H. M., Ward, J. M., and Stinson S. F. Morphology of nasal-cavity tumors in rats after chronic inhalation of 1,2-dibromo-3-chloropropane. Br. J. Cancer 42: 772–781 (1980).
39. Vidić, B., and Greditzer, H. The histochemical and microscopical differentiation of the respiratory glands around the maxillary sinus of the rat. Am. J. Anat. 132–491–514 (1971).
40. Marks, S. C. Pathogenesis of osteopetrosis in the *ia* rat: reduced bone resorption due to reduced osteoclast function. Am. J. Anat. 138: 165–190 (1973).
41. Stewart, H. L., Dunn, T. B., Snell, K. C., and Deringer, M. K. Tumors of the respiratory tract. In: Pathology of Tumors in Laboratory Animals, Vol. II (V. S. Turusov, Ed.), IARC Scientific Publications, Lyon, 1979, pp. 251–252.
42. Morgan, K. T., Monticello, T. M., Fleischman, A., and Patra, A. L. Preparation of rat nasal airway casts and their application to studies of nasal airflow. In: Extrapolation of Dosimetric Relationships for Inhaled Particles and Gases, Chapter 5 (A. W. Hayes and J. D. Crapo, Eds.), Academic Press, Inc., Orlando, FL, 1989.
43. Robins, M. W., and Rowlatt, C. Dental abnormalities in aged mice. Gerontologia 17: 261–272 (1971).

PLATE 1. Nasal vestibule with erosion and ulceration of the squamous epithelial lining of the dorsal wall and lateral aspect of atrioturbinate.

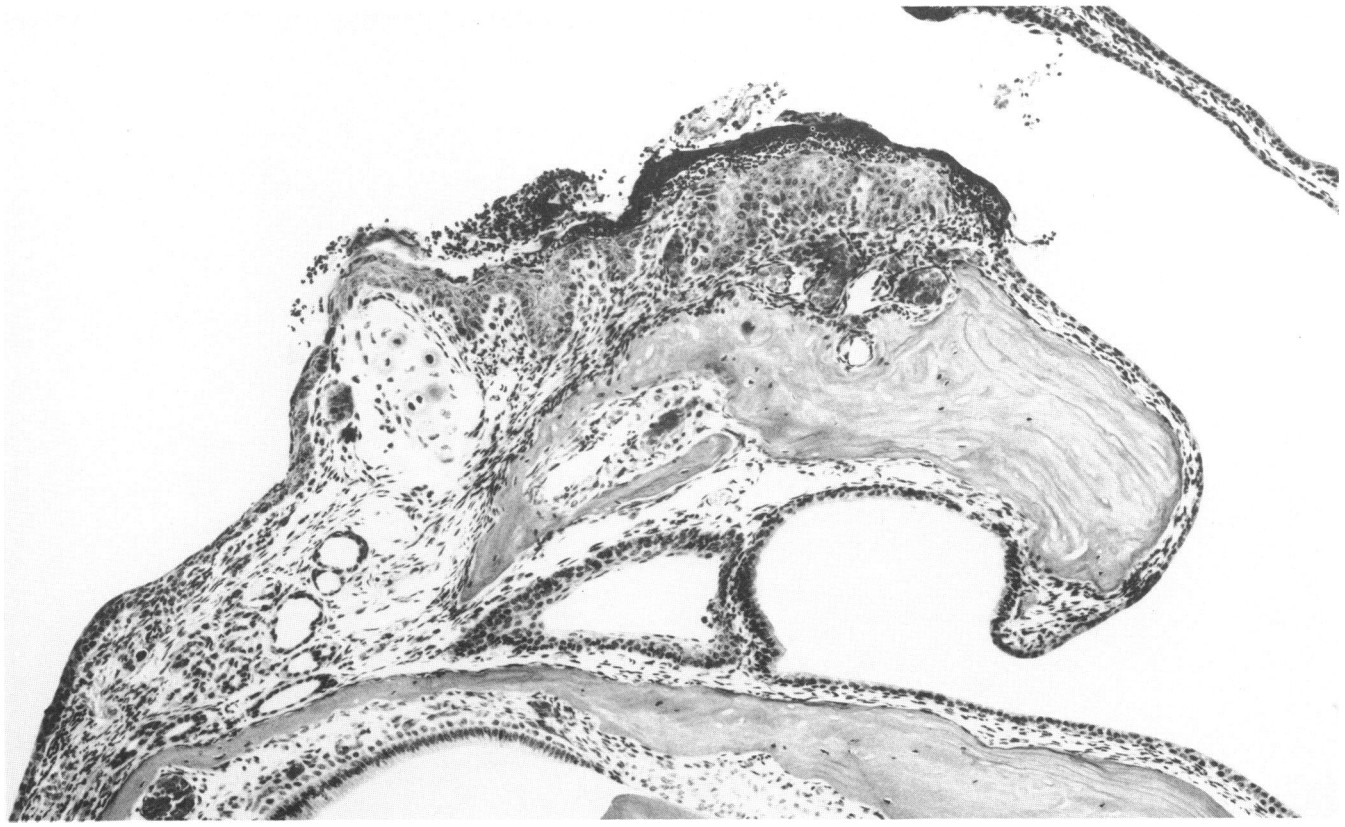

PLATE 2. Epithelial hyperplasia resulting in rete-ridge formation.

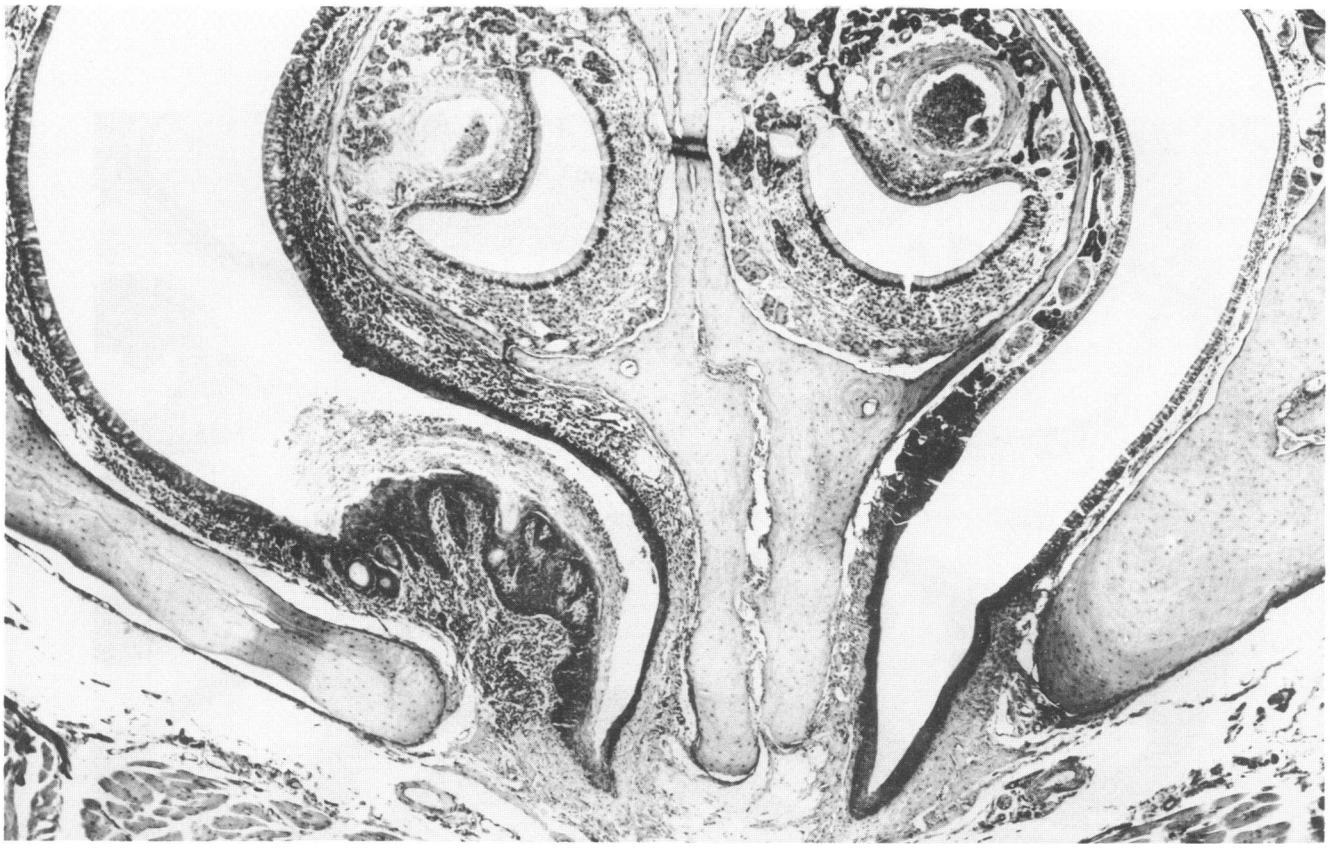

PLATE 3. Focal epithelial hyperplasia confined to the ventral meatus.

PLATE 4. Incisive ducts lined by squamous epithelium.

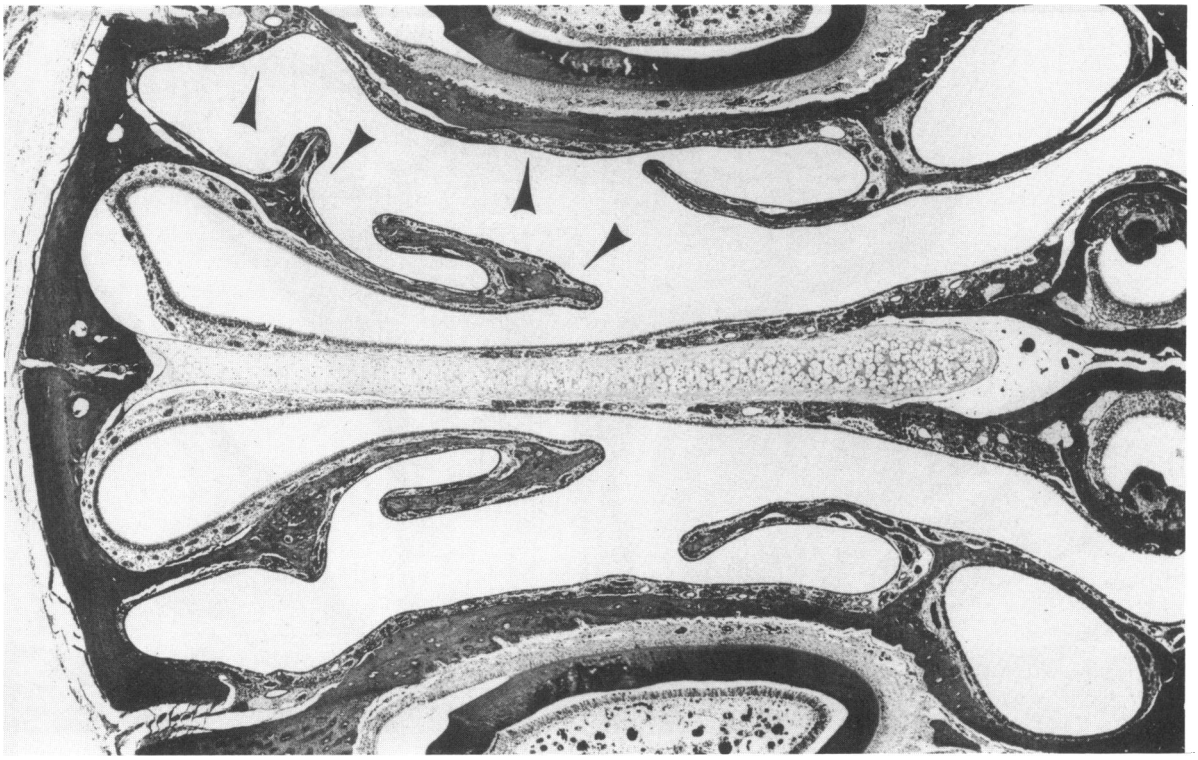

PLATE 5. Cross-section of rat nasal cavity at the level of the lateral scroll of the nasoturbinate. The lateral wall and lateral aspect of nasoturbinate (indicated by arrowheads), is lined by a low pseudostratified epithelium having a cuboidal appearance.

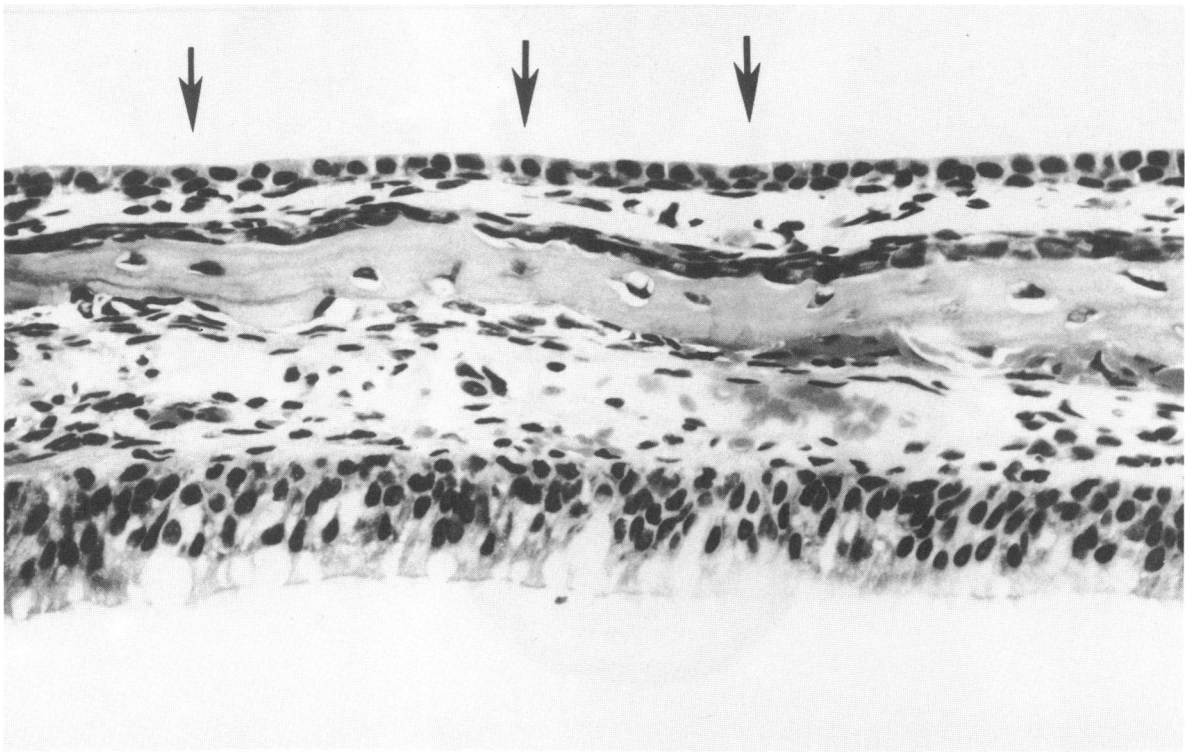

PLATE 6. Nasoturbinate from a control animal. The lateral aspect (arrows) is lined by a low pseudostratified epithelium having a cuboidal appearance, while the medial aspect is covered by pseudostratified ciliated columnar epithelium.

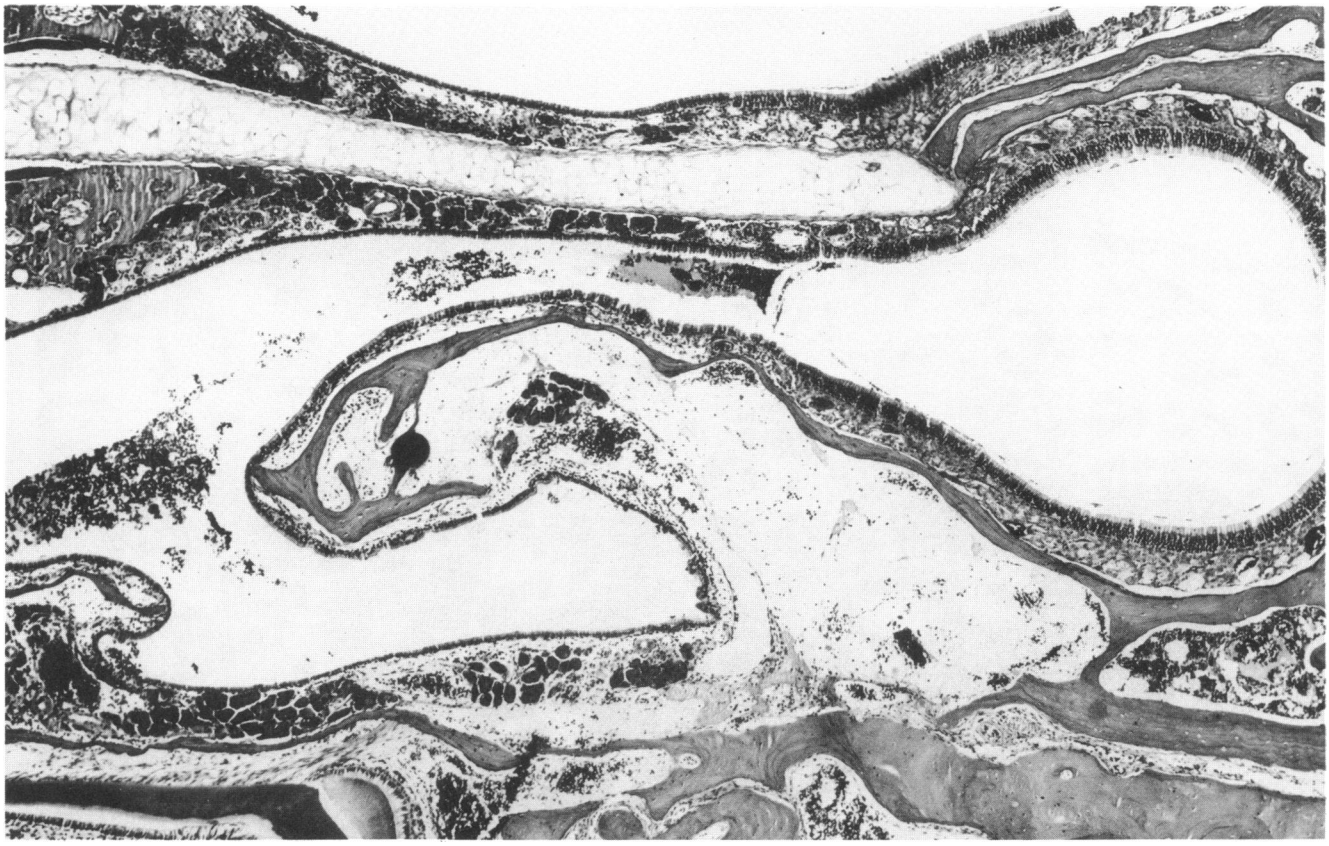

PLATE 7. Nasoturbinate distended by edema of the lamina propria. Some free red cells are present in the nasal lumen.

PLATE 8. Suppurative rhinitis. A neutrophilic exudate fills the airway lumen.

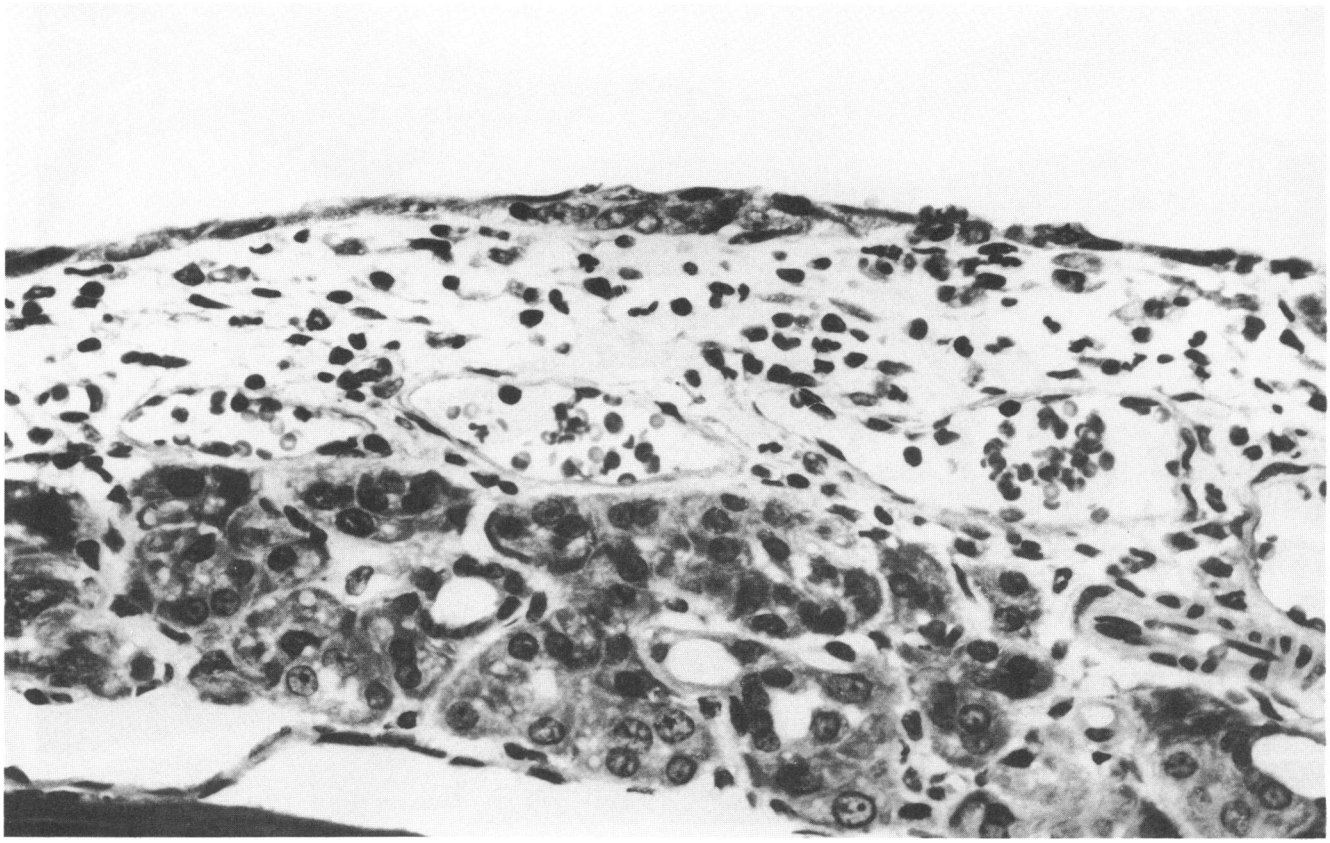

PLATE 9. Erosion of the cuboidal epithelial cell lining the lateral wall.

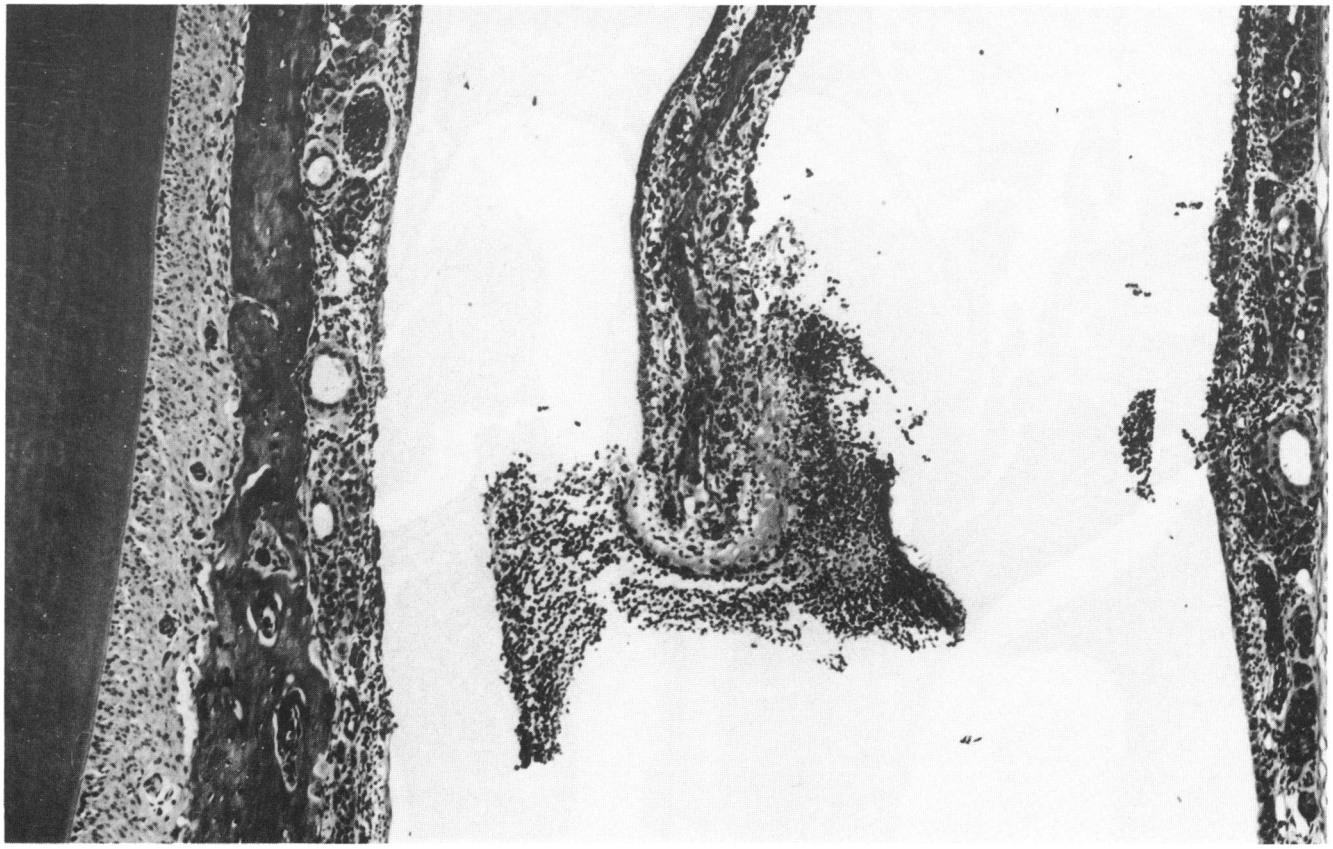

PLATE 10. Ulceration of the nasoturbinate epithelium with an overlying serocellular exudate.

PLATE 11. Adhesion of the nasoturbinate to the lateral wall.

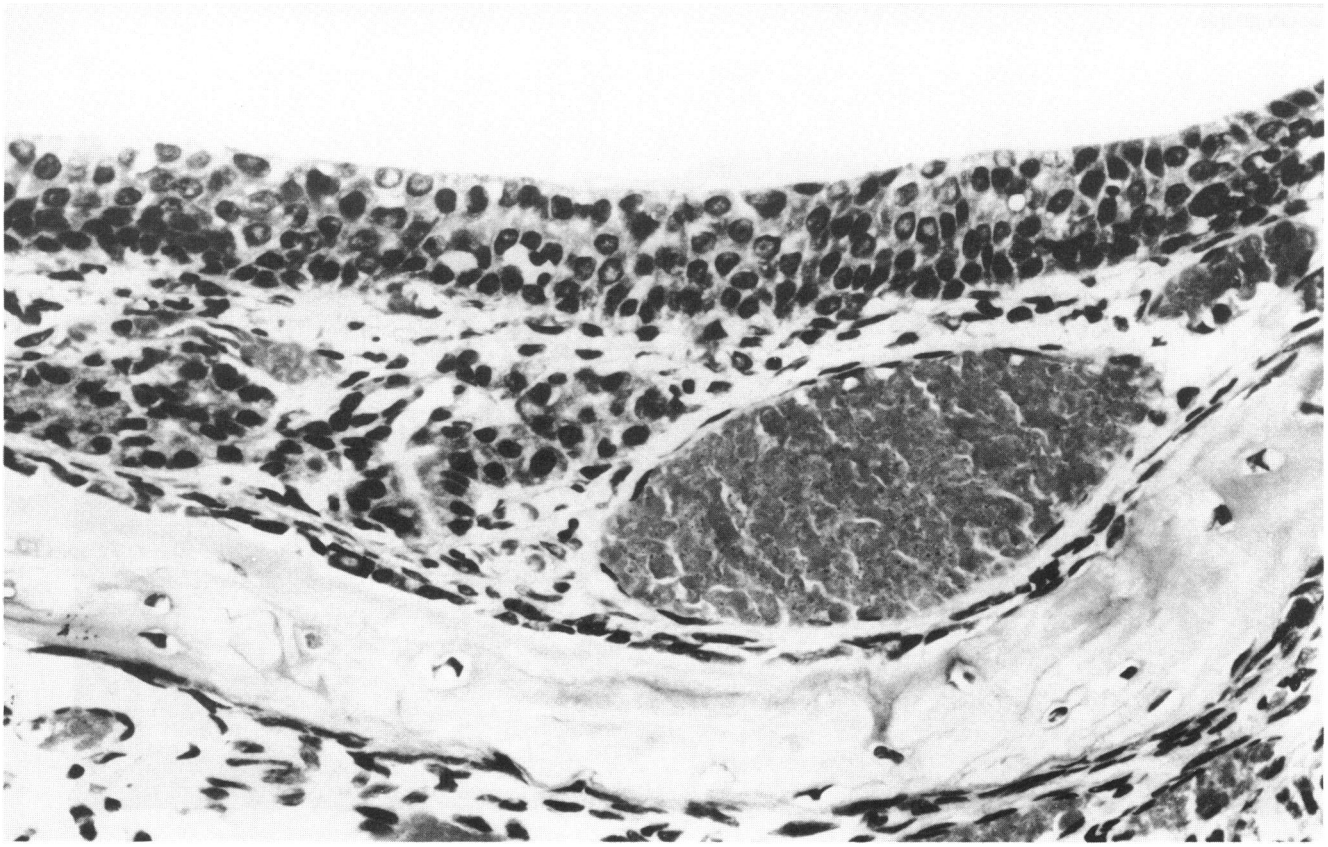

PLATE 12. Hyperplasia of the epithelium lining the lateral wall.

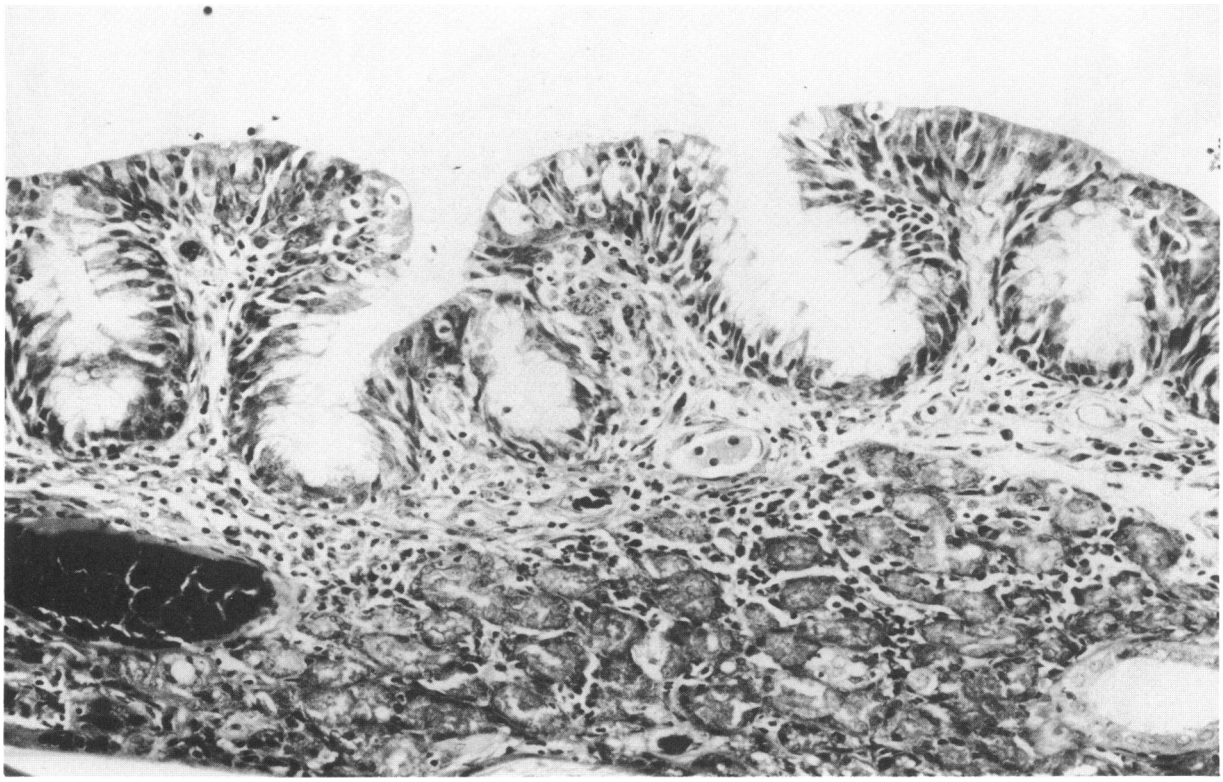

PLATE 13. Secretory and respiratory epithelial cell hyperplasia of the nasal septum. Note mucosal folding and the formation of pseudoglands.

PLATE 14. Epithelial hyperplasia and early squamous metaplasia with a mixed inflammatory cell infiltrate in the lamina propria. Accumulation of inflammatory cells in intraepithelial vacuoles result in the formation of microabscesses.

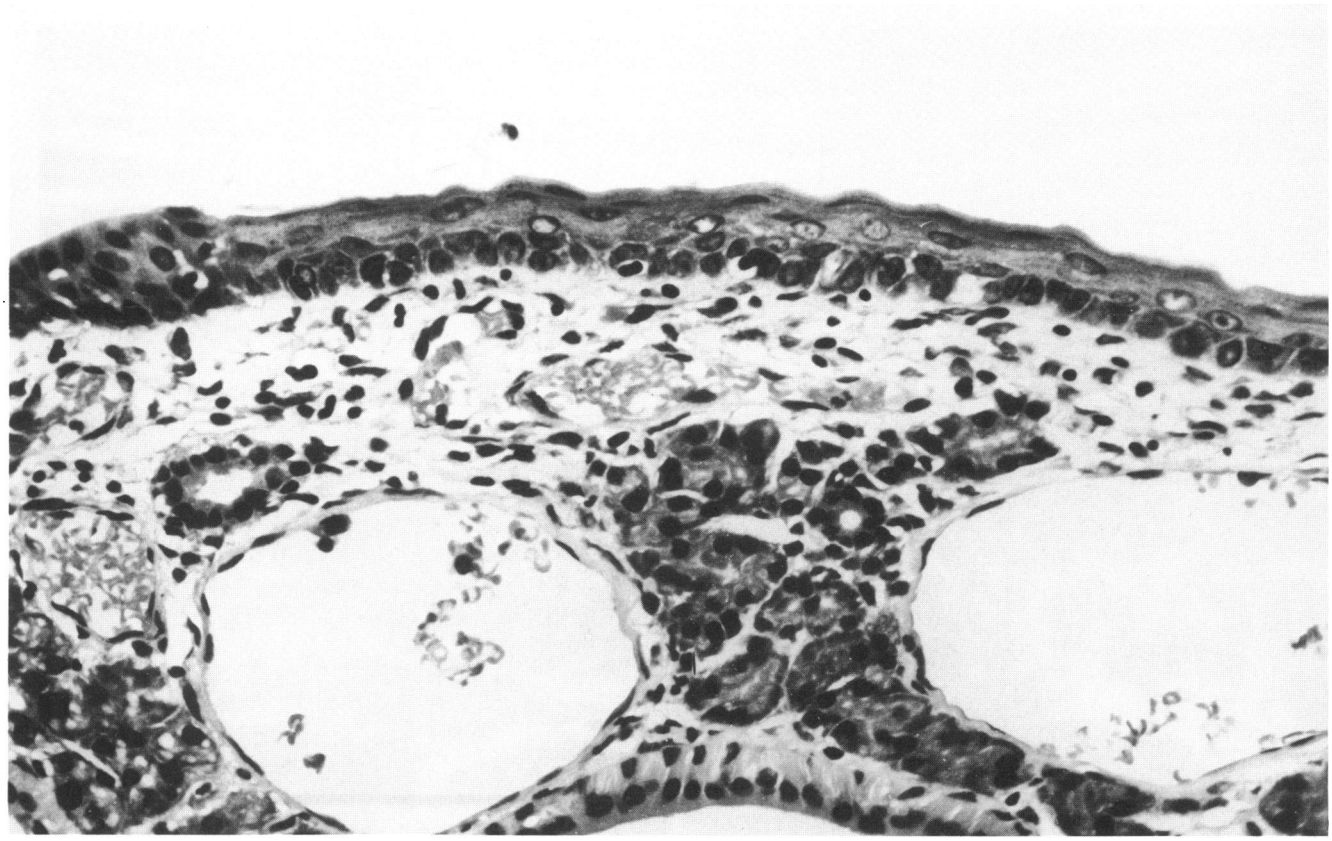

PLATE 15. Squamous metaplasia of the epithelium lining the lateral wall.

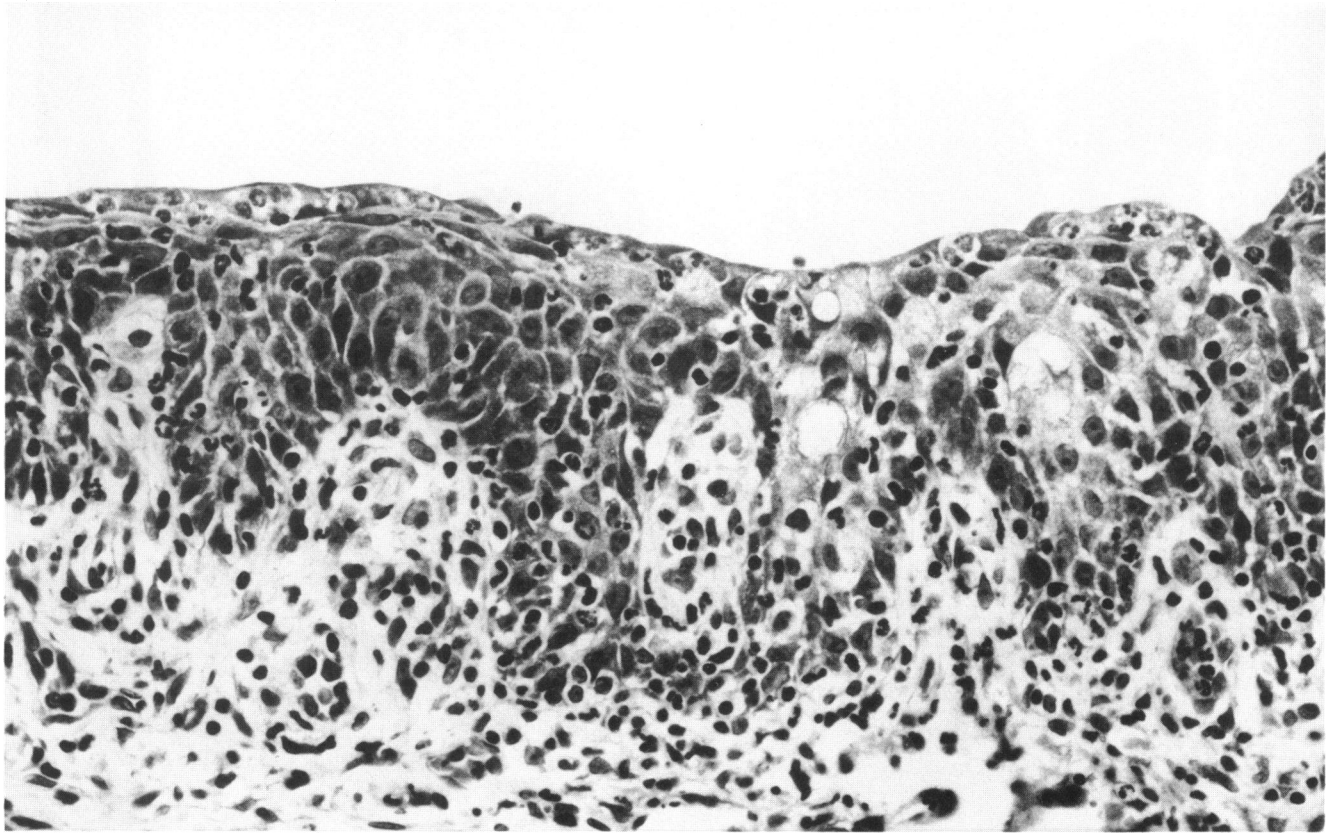

PLATE 16. Epithelial hyperplasia and adaptive squamous metaplasia of the respiratory epithelium.

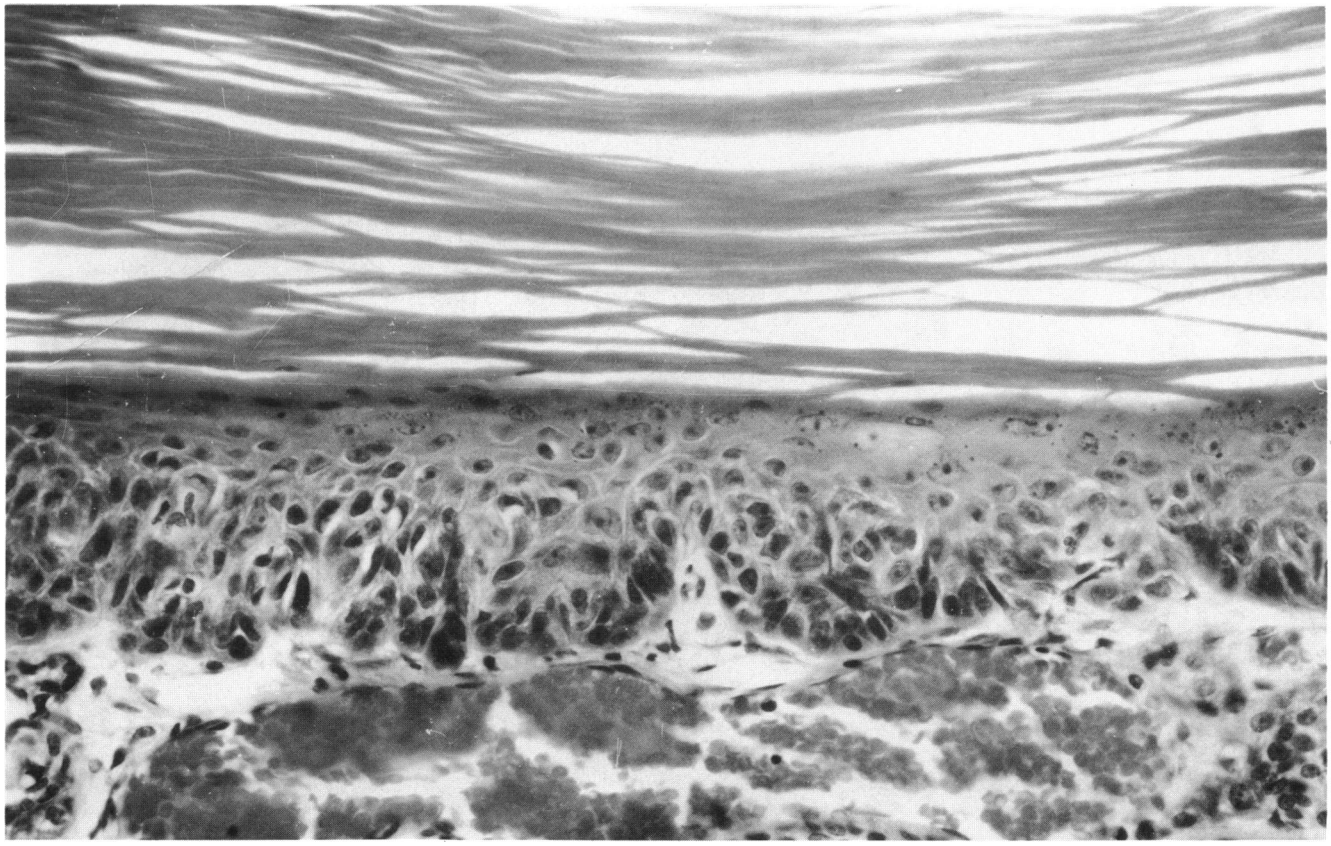

PLATE 17. Epithelial hyperplasia, metaplasia, and keratinization of the nasal mucosa exposed to an irritant gas.

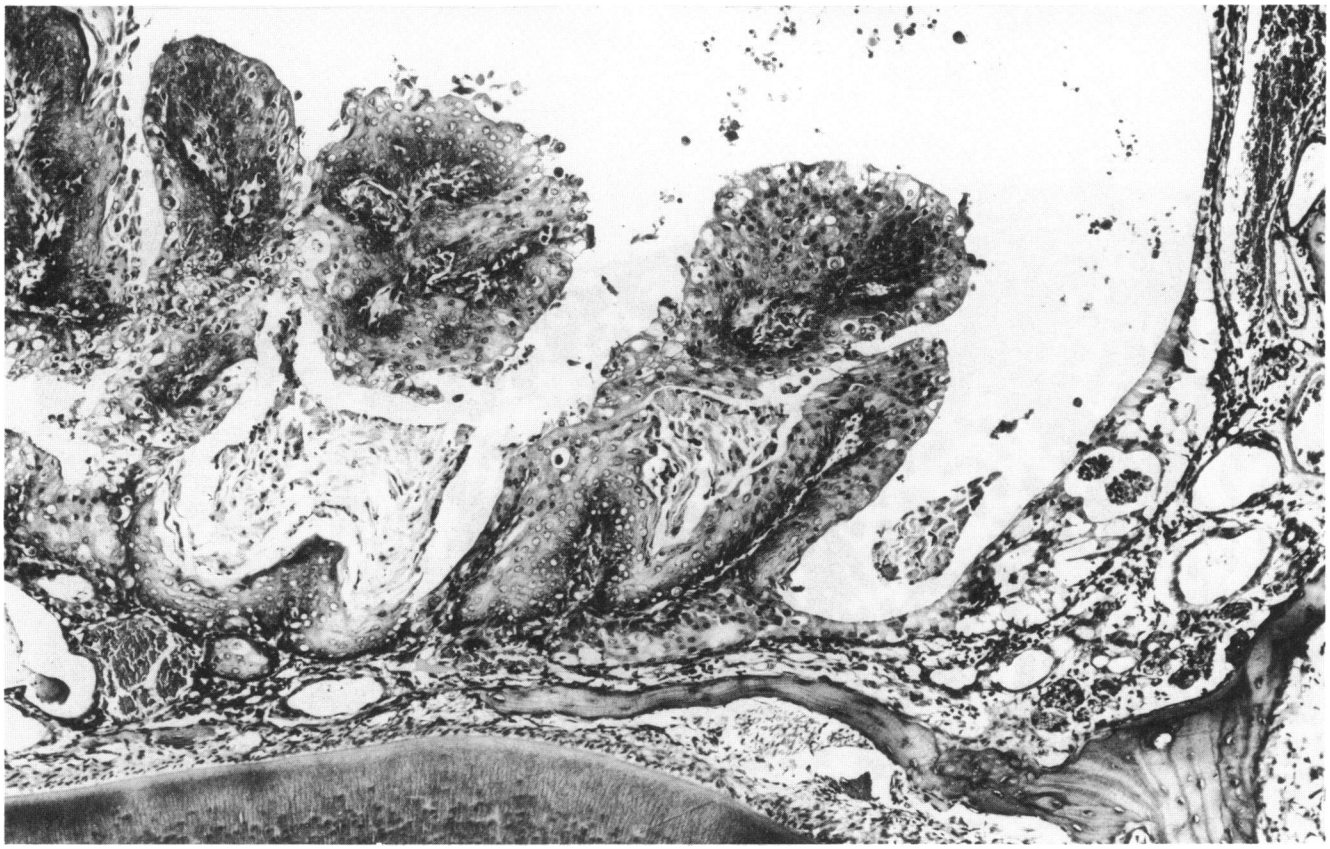

PLATE 18. Dysplasia of the epithelium of the lateral wall.

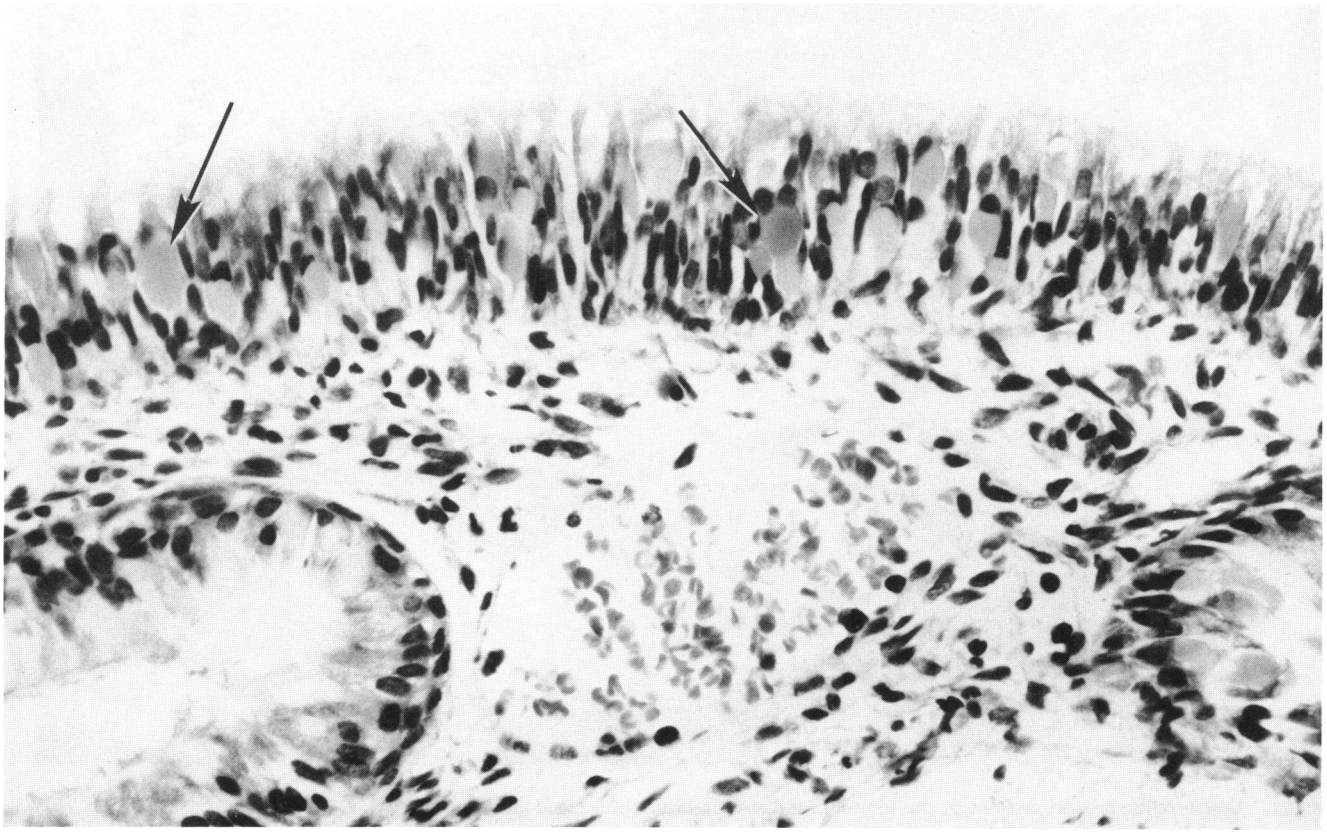

PLATE 19. Eosinophilic globules (arrows) present in respiratory epithelial cells.

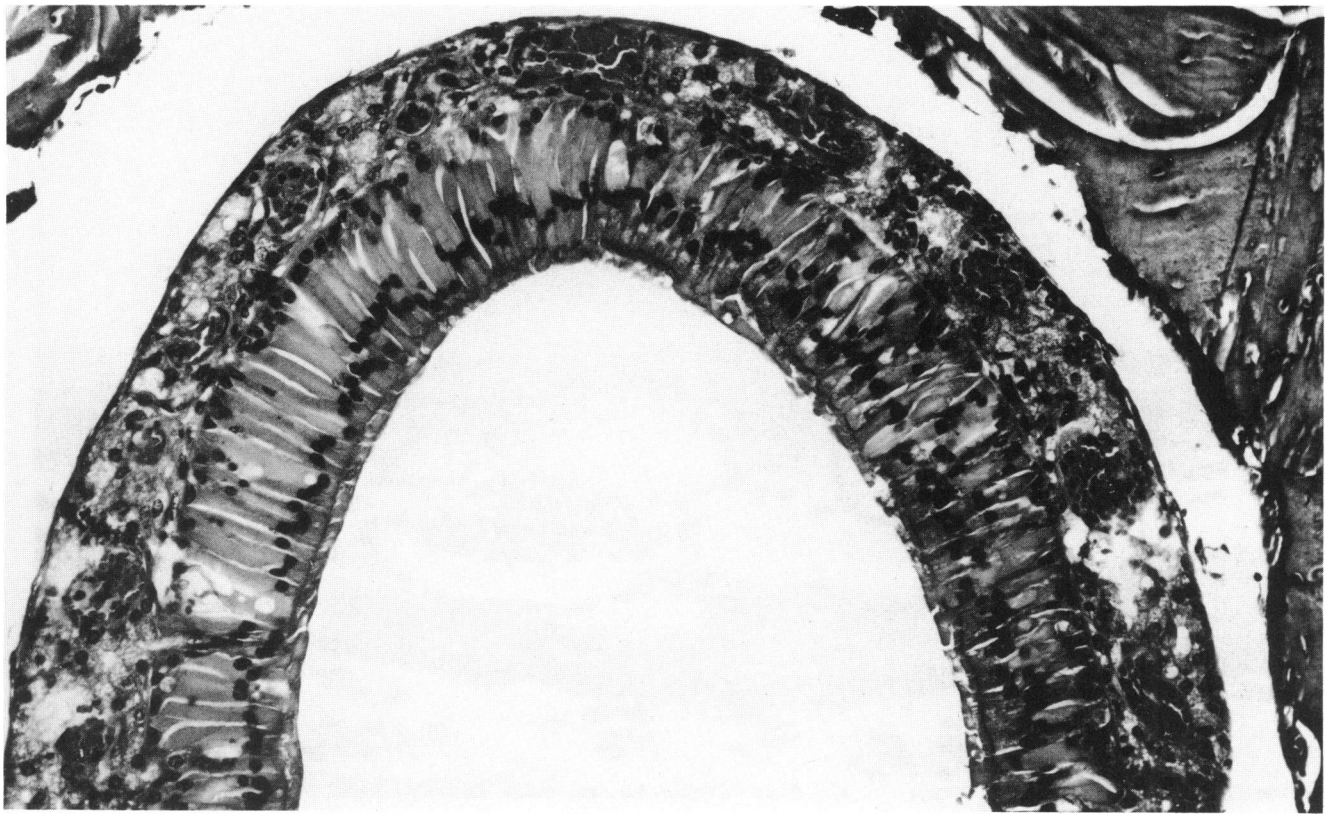

PLATE 20. Eosinophilic globules distend sustentacular cells of the olfactory mucosa.

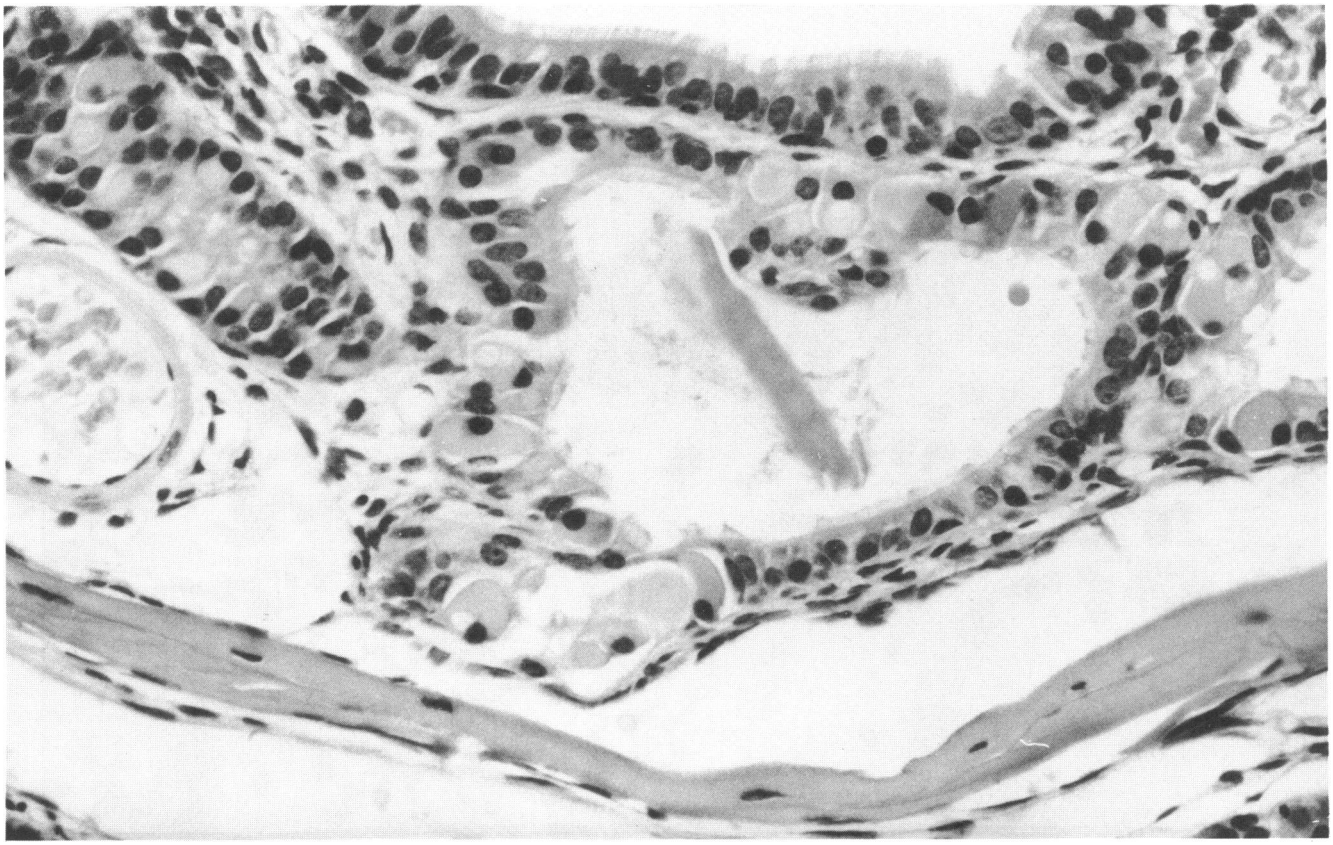

PLATE 21. Eosinophilic crystal present in the lumen of a distended duct of a nasal gland.

PLATE 22. Multiple corpora amylacea associated with the basement membrane of the respiratory epithelium of a control rat.

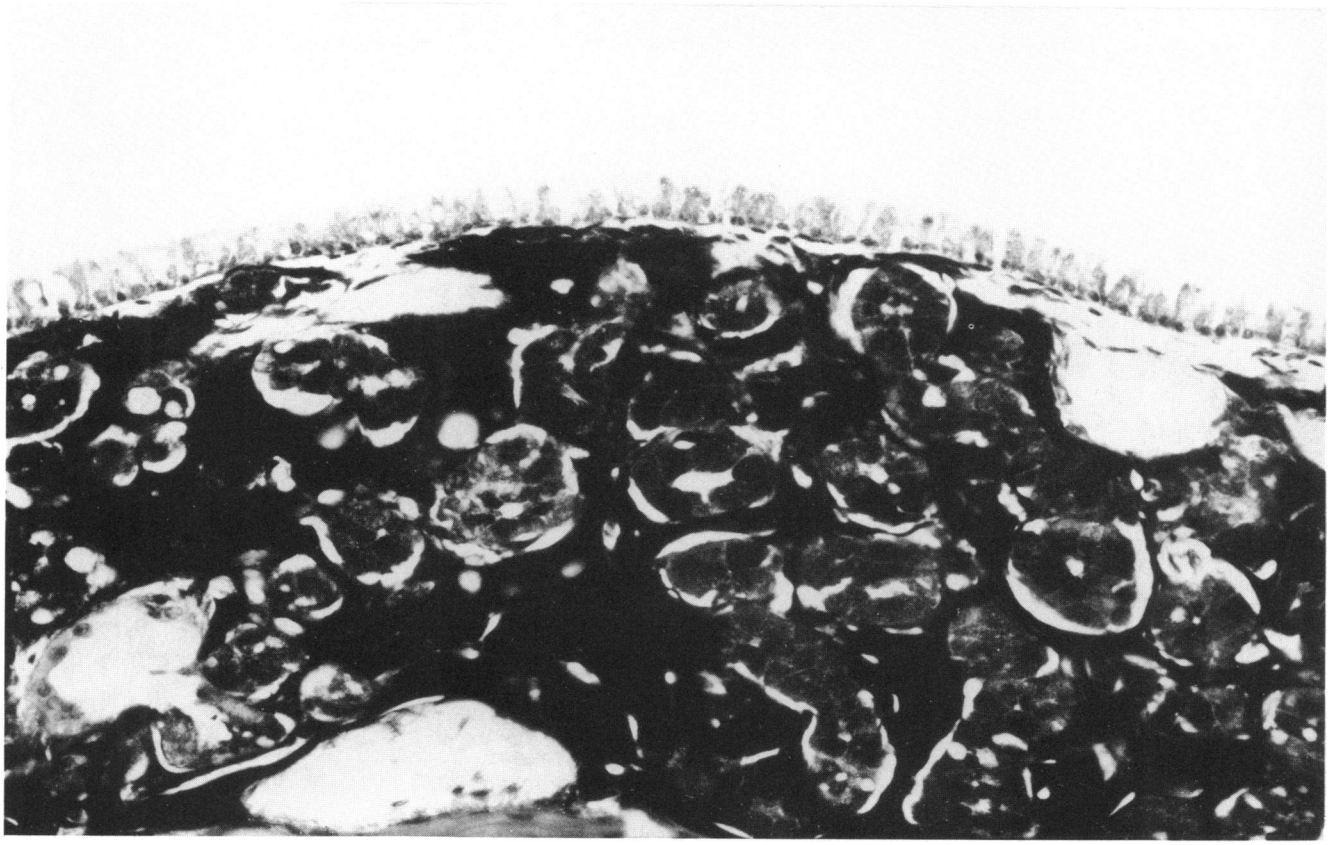

PLATE 23. Ventral septal area of a control mouse. Homogeneous PAS-positive material distends the lamina propria.

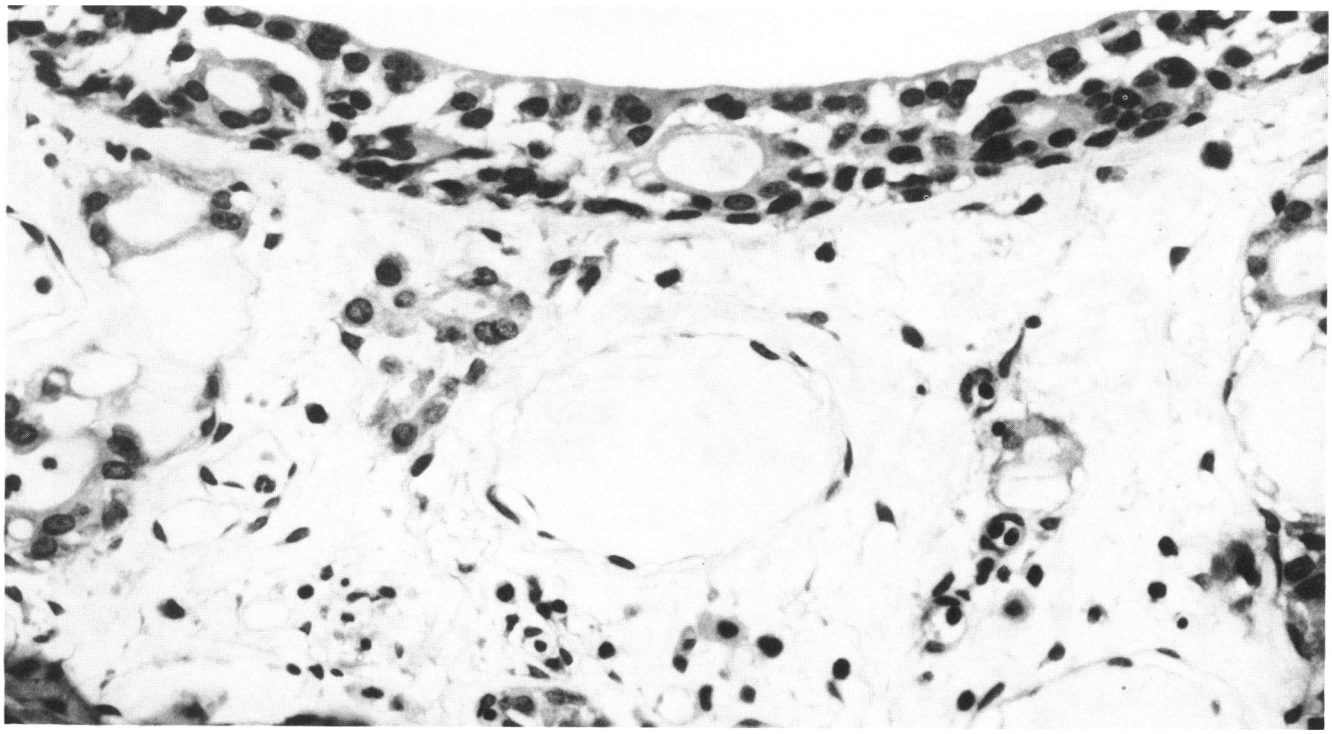

PLATE 24. Atrophy of the olfactory epithelium. Also note the loss of olfactory nerve bundles in the lamina propria.

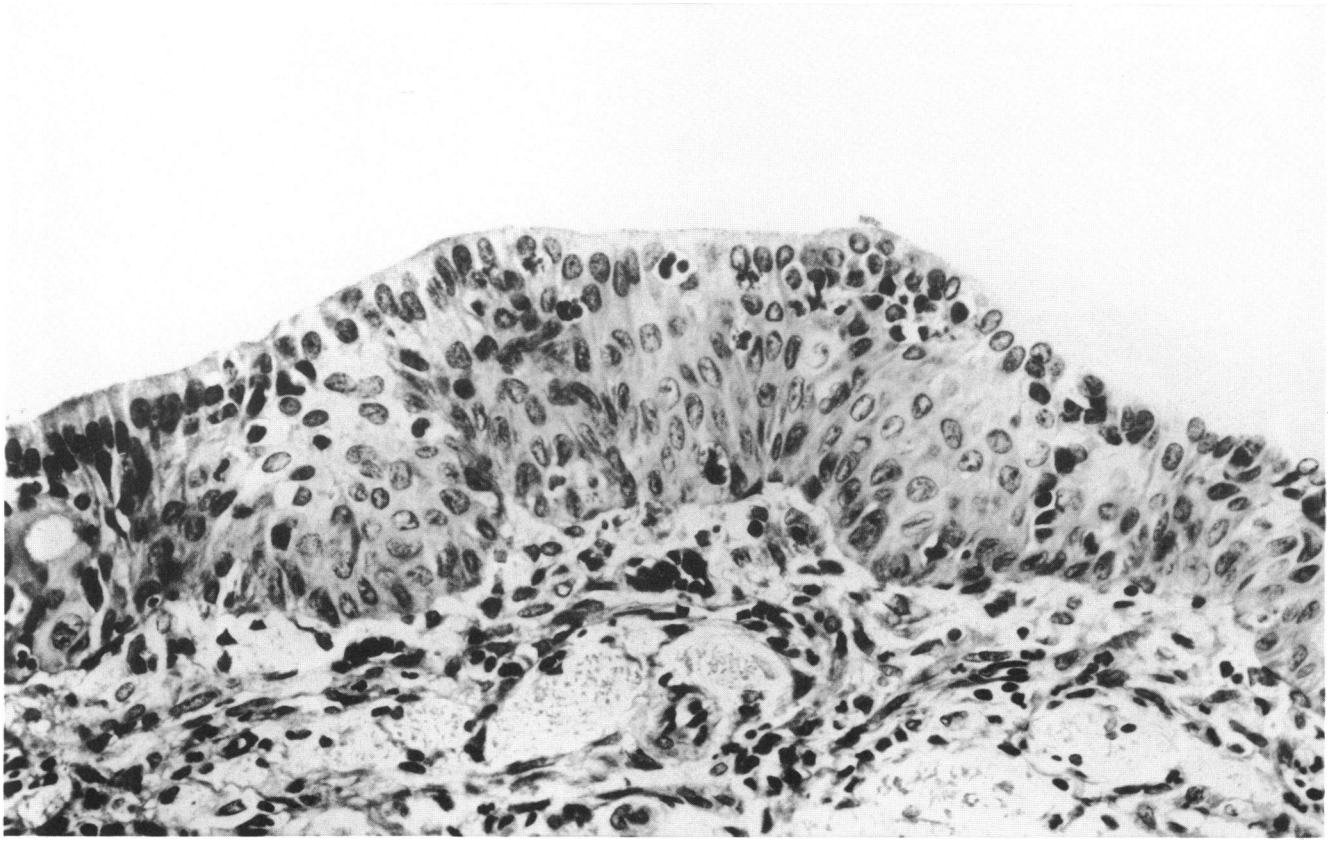

PLATE 25. Metaplasia of the olfactory epithelium presumed to be a result of basal cell hyperplasia.

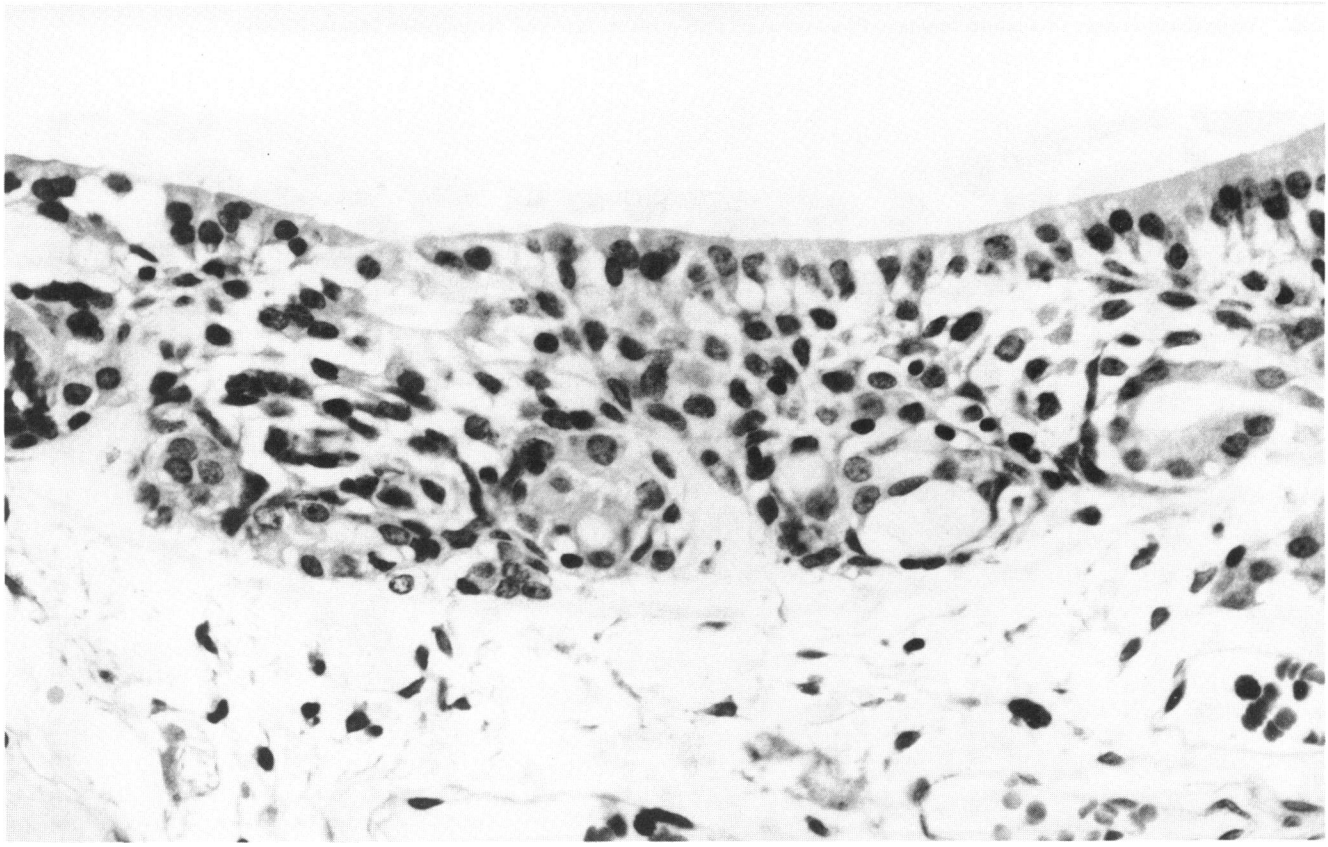

PLATE 26. Focal hyperplasia of basal cells in the olfactory epithelium forming intraepithelial rosettelike structures.

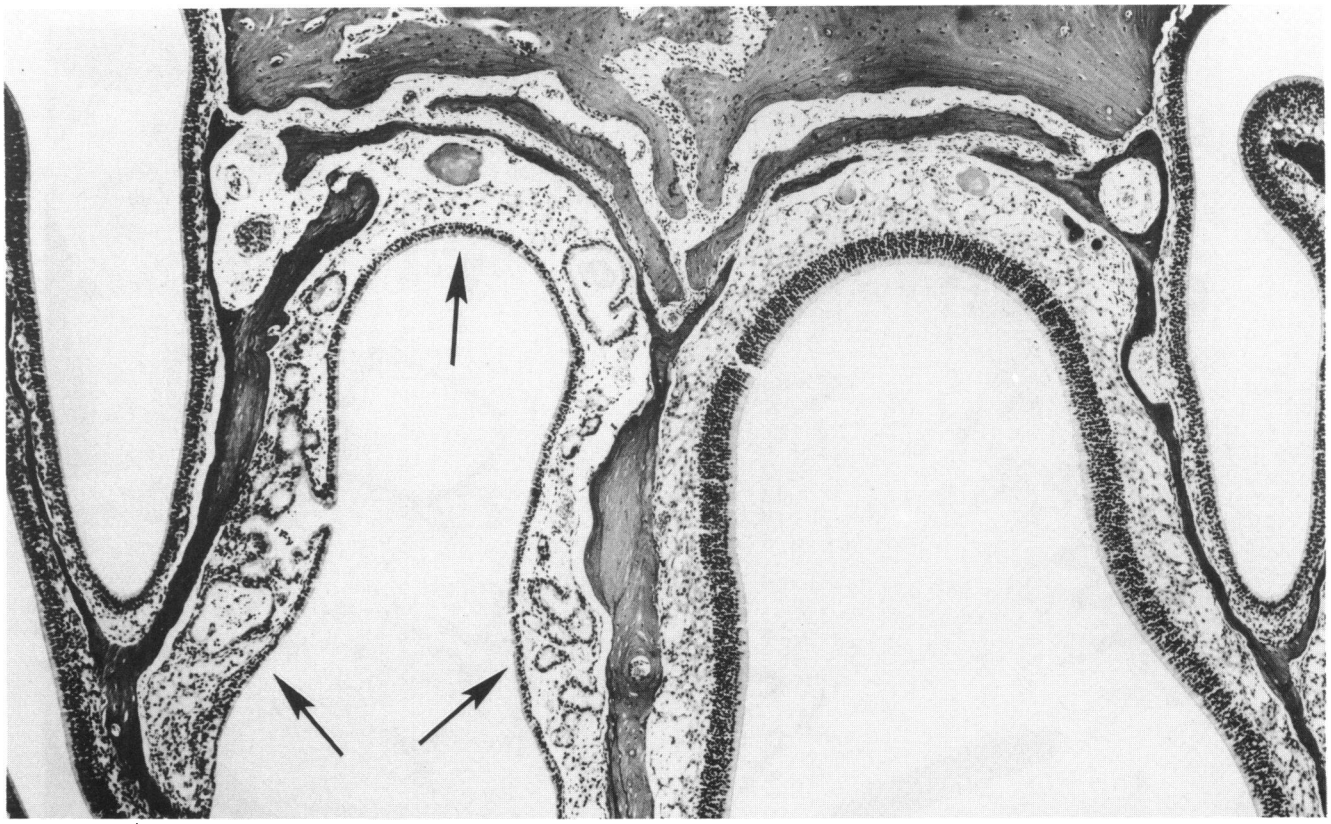

PLATE 27. Unilateral respiratory metaplasia (arrows) of the olfactory epithelium. The contralateral side is lined by normal olfactory epithelium.

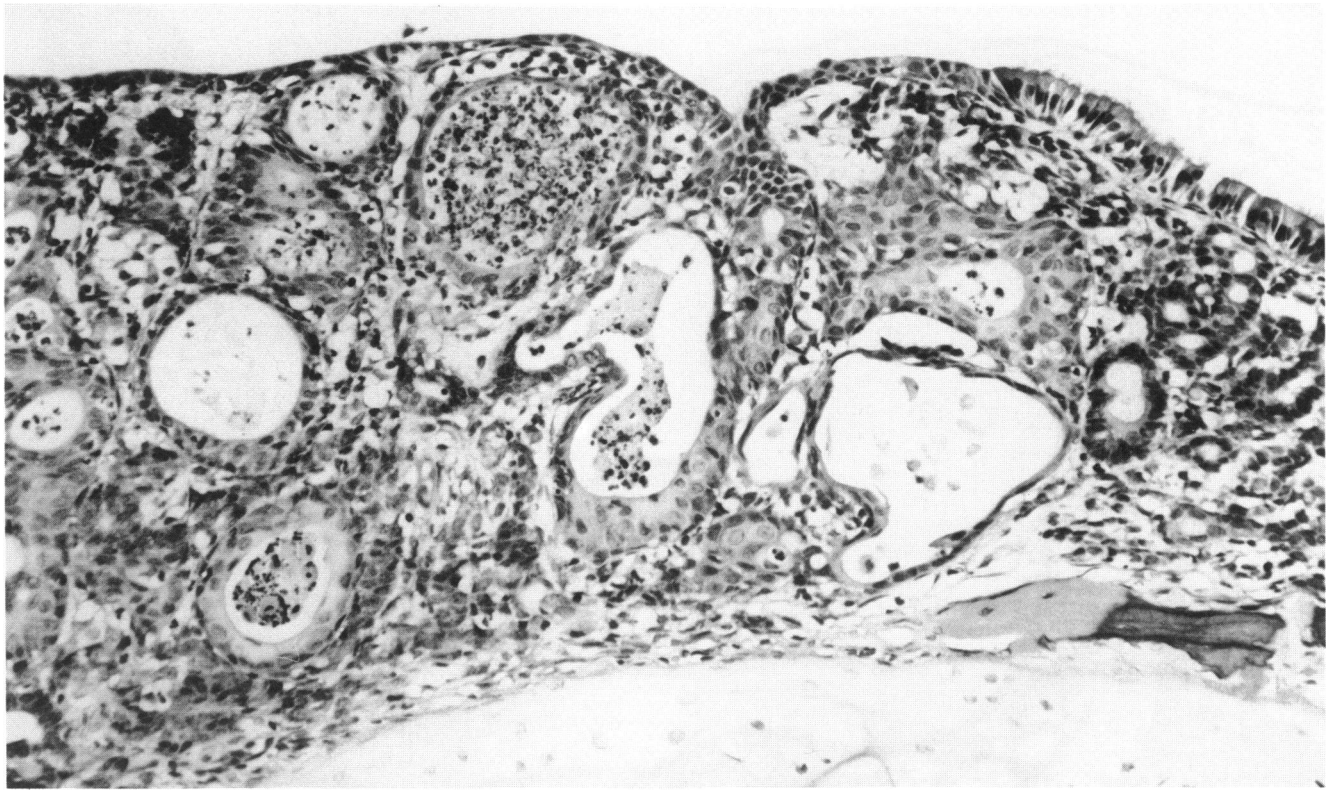

PLATE 28. Glandular distension, plugging of ducts by inflammatory cells, and squamous metaplasia of many nasal glands.

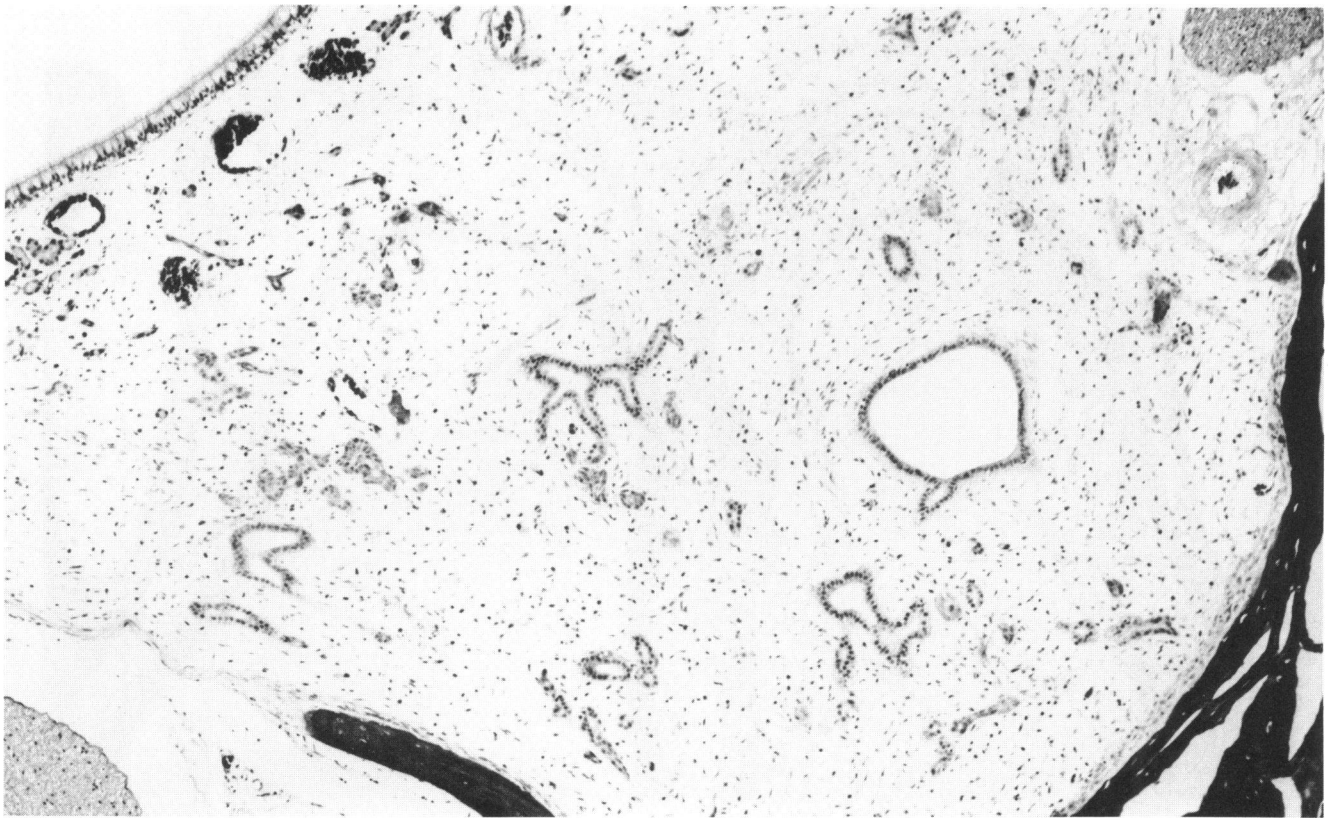

PLATE 29. Severe atrophy and necrosis of Steno's gland following the administration of a toxic compound. Only a few ducts of these nasal glands remain.

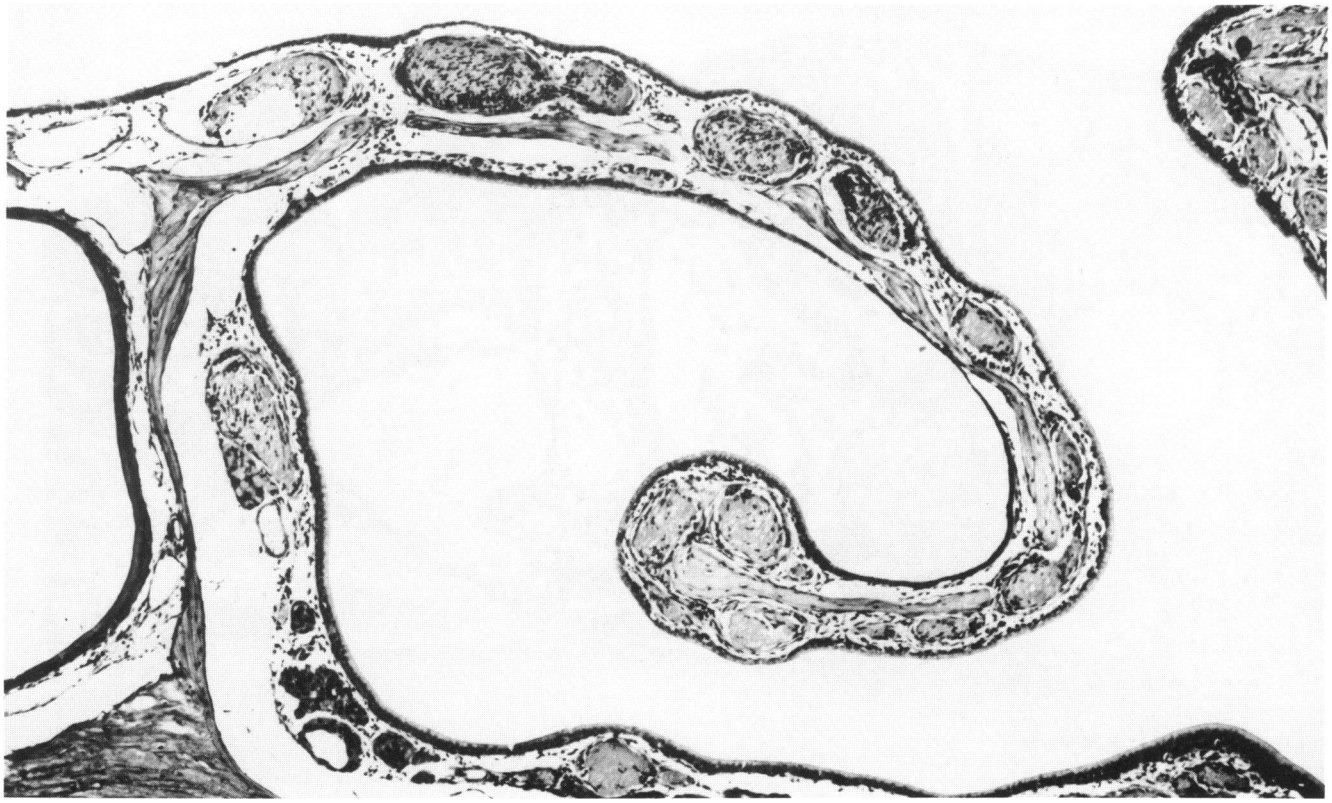

PLATE 30. Thrombosis of vessels in the maxilloturbinate.

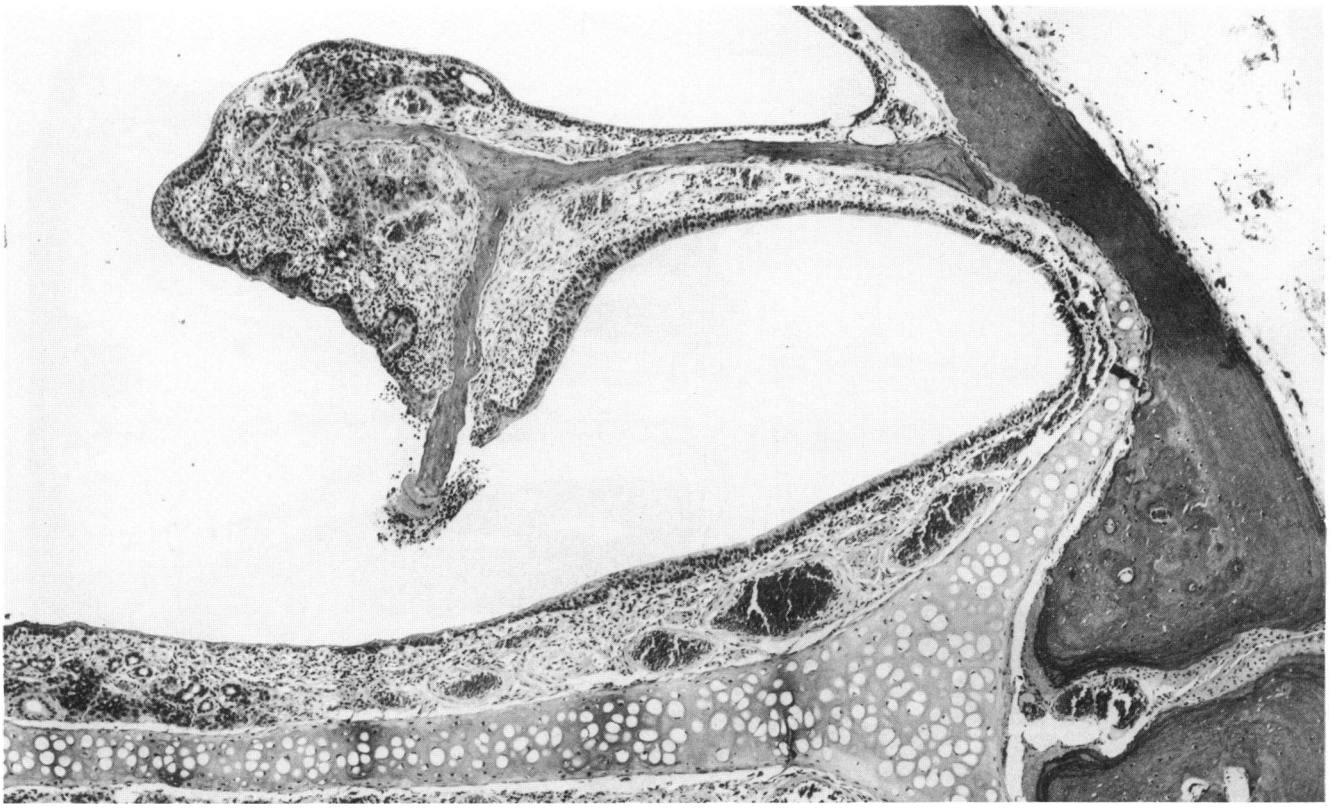

PLATE 31. Necrosis of nasoturbinate bone that protrudes through the overlying epithelium into the lumen.

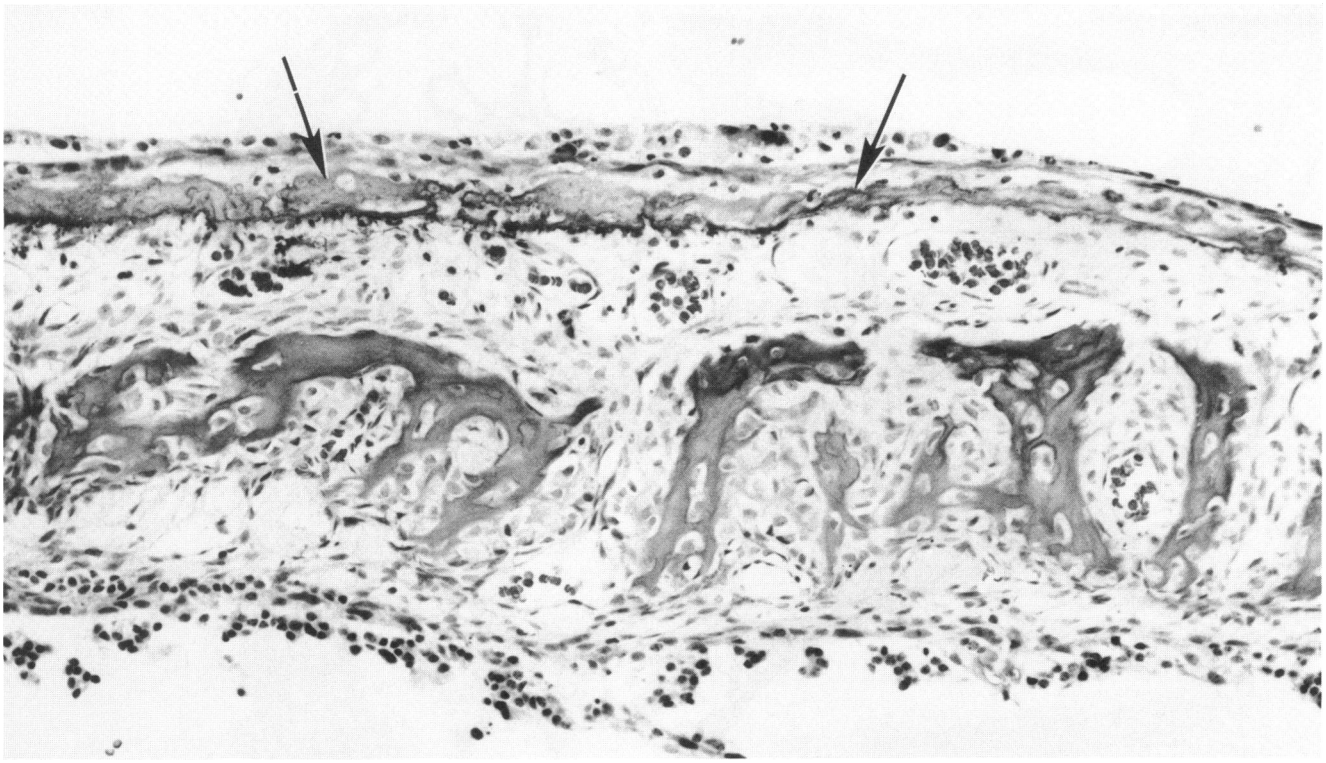

PLATE 32. Osteofibrosis of the ethmoid turbinate bone. Note the proliferation of osteoprogenitor of fibroblastlike cells near the periosteal surface. In addition, there is mineralization or the epithelial basement membrane (arrows) and loss of the olfactory mucosa.

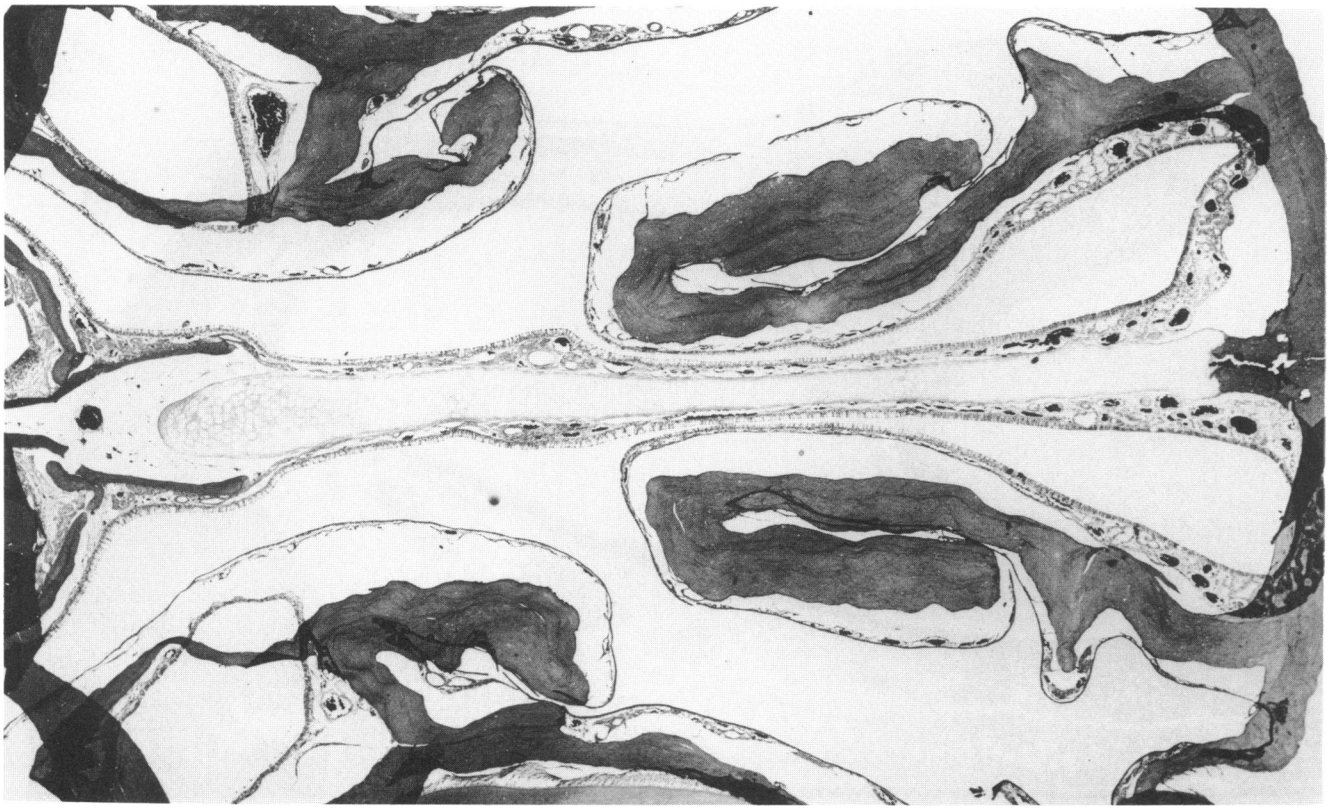

PLATE 33. Osteopetrosis of the skull and turbinate bones. Note the marked thickening of the naso- and maxilloturbinates with an associated atrophy of the nasal mucosa.

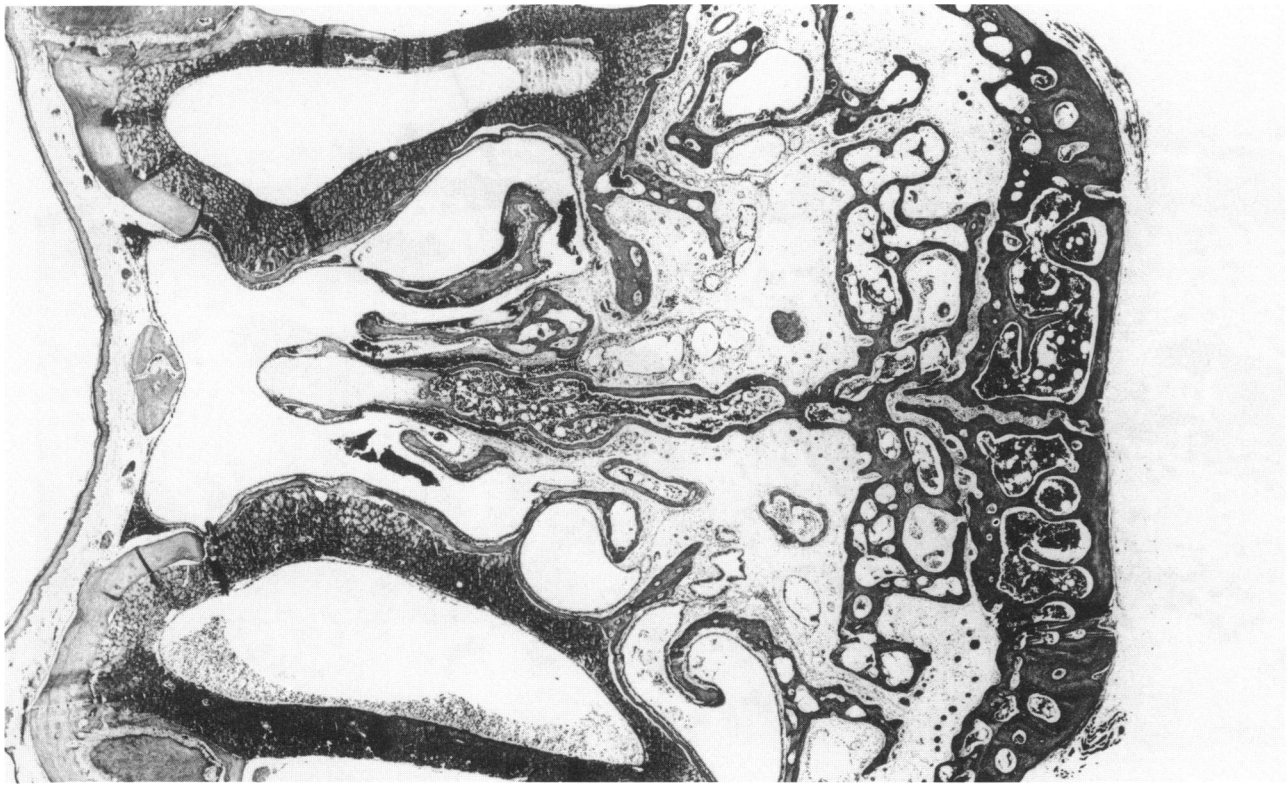

PLATE 34. Section of ethmoid turbinates taken at the level of the septal window demonstrating extensive remodeling of the turbinates following olfactory epithelial necrosis.

PLATE 35. Vomeronasal organ (Jacobson's organ) of a control rat.

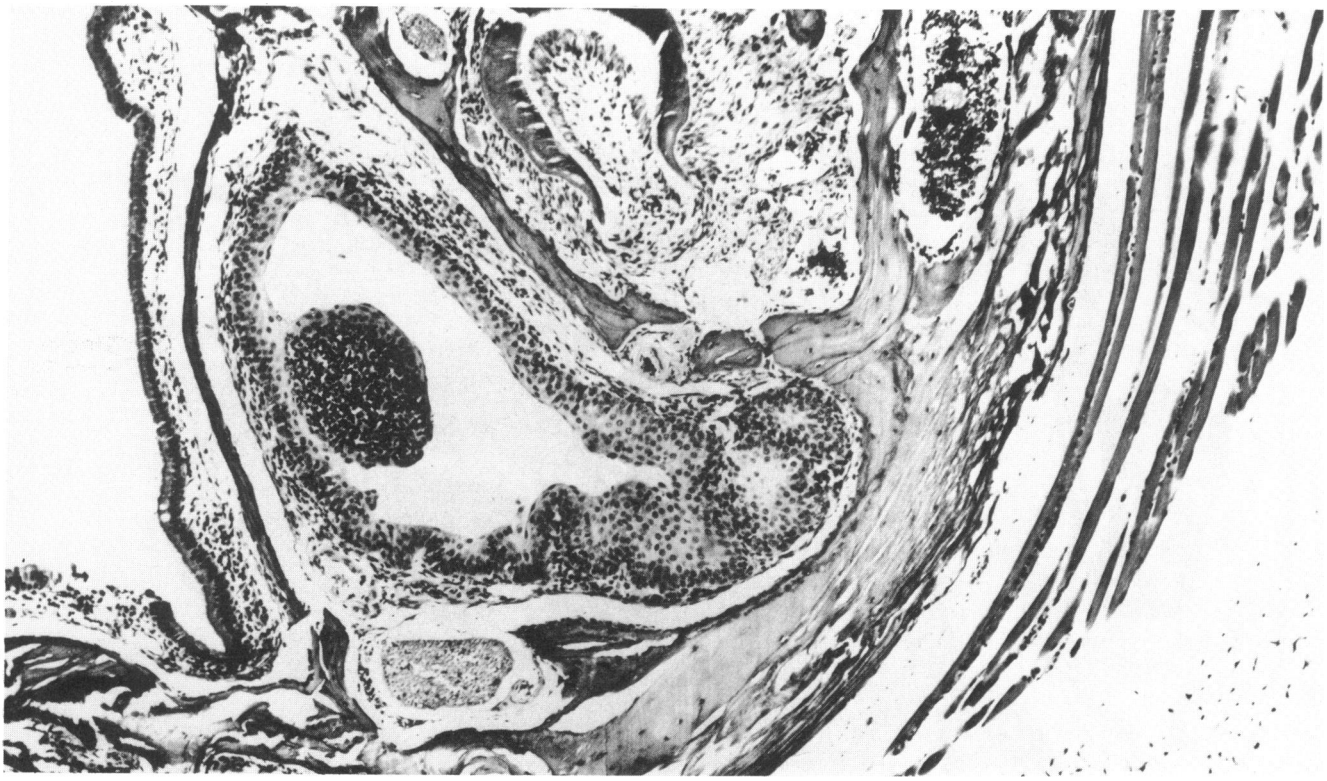

PLATE 36. Nasolacrimal duct ventromedial to the root of the incisor tooth in the nasal vestibule. There is hyperplasia and metaplasia of the epithelial lining and an intraepithelial lymphoid aggregate protruding into the duct lumen.

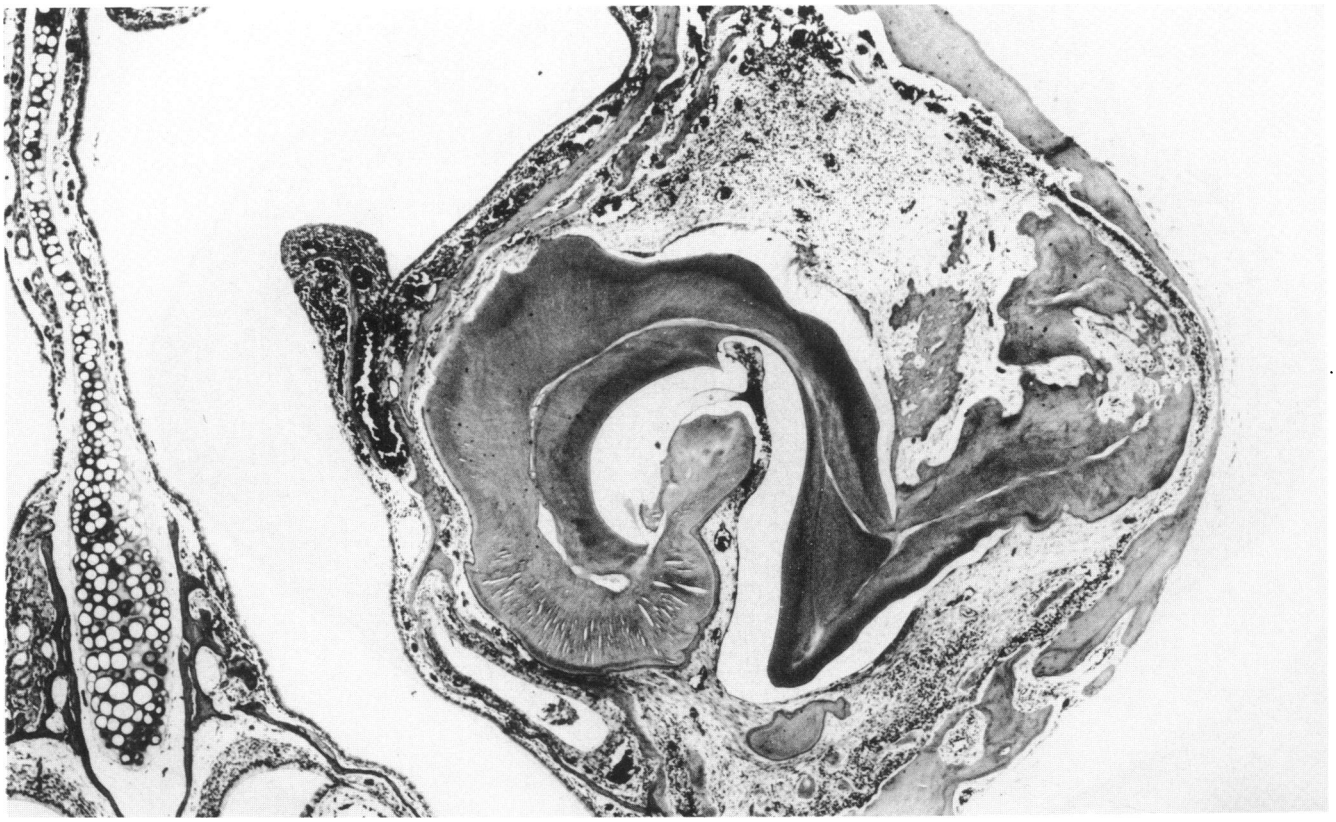

PLATE 37. Dental dysplasia (odontodysplasia) of the incisor tooth.

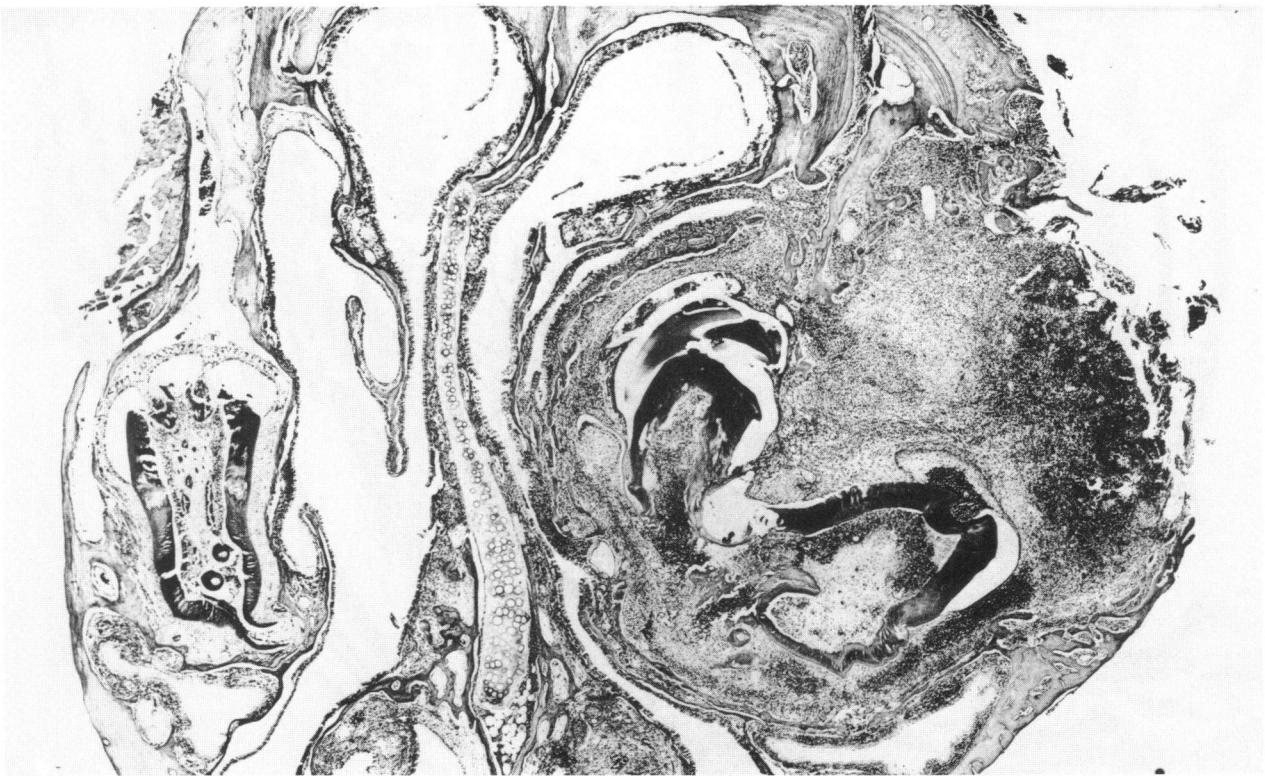

PLATE 38. Dysplastic incisor tooth surrounded by inflammatory cells and exhibiting areas of necrosis. Note partial occlusion of the nasal passages.